Molecular Magnetism

International Edition: DOI: 10.1002/anie.201502730
German Edition: DOI: 10.1002/ange.201502730

Heterometallic Rings: Their Physics and use as Supramolecular Building Blocks

*Eric J. L. McInnes, Grigore A. Timco, George F. S. Whitehead, and Richard E. P. Winpenny**

Keywords:
carboxylate clusters · heterometallic rings · metallocycles · molecular magnets · supramolecular chemistry

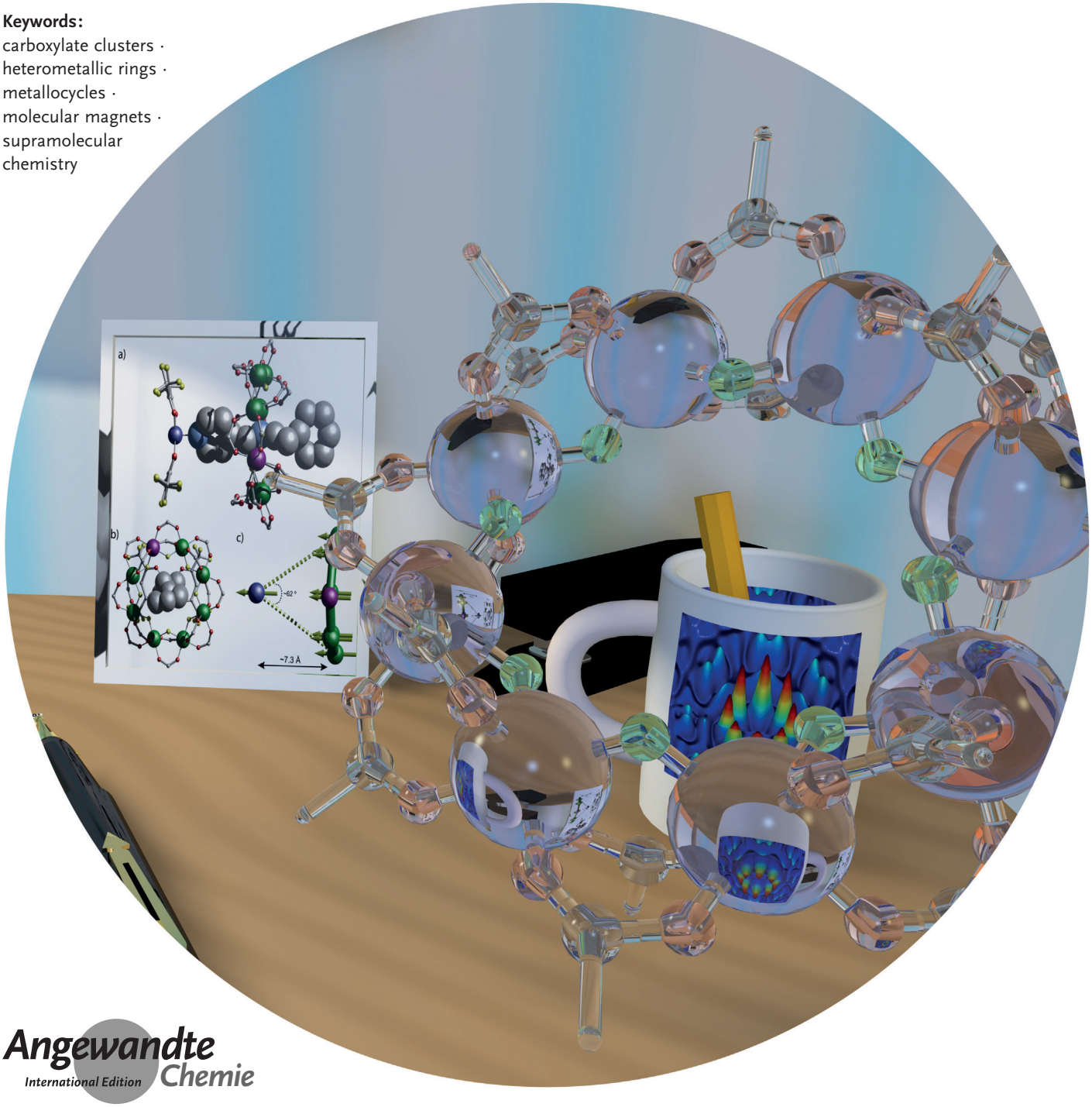

An enormous family of heterometallic rings has been made. The first were Cr_7M rings where $M = Ni^{II}$, Zn^{II}, Mn^{II}, and rings have been made with as many as fourteen metal centers in the cyclic structure. They are bridged externally by carboxylates, and internally by fluorides or a penta-deprotonated polyol. The size of the rings is controlled through templates which have included a range of ammonium or imidazolium ions, alkali metals and coordination compounds. The rings can be functionalized to act as ligands, and incorporated into hybrid organic–inorganic rotaxanes and into molecules containing up to 200 metal centers. Physical studies reported include: magnetic measurements, inelastic neutron scattering (including single crystal measurements), electron paramagnetic resonance spectroscopy (including measurements of phase memory times), NMR spectroscopy (both solution and solid state), and polarized neutron diffraction. The rings are hence ideal for understanding magnetism in elegant exchange-coupled systems.

From the Contents

1. Homometallic Rings: A Brief History

Physicists view molecules very differently to chemists. These different viewpoints can be easily seen in molecular magnetism; for a physicist the ideal magnetic molecule has a simple arrangement of magnetic centers, which will allow a simple Hamiltonian to be used to model the magnetic data and to test a physical hypothesis. A chemist might, on the other hand, want to make an elaborate magnetic molecule, with multiple different spin centers of several types, and might delight in introducing new ligand types to achieve new structural types. Such unnecessary baroque elaboration can seem frivolous to the more classically minded physicist.

Therefore when chemists learnt how to make cyclic polymetallic compounds they produced magnetic molecules that also appealed to physicists. The first significant study of such a compound was of $[Fe(OMe)_2(O_2CCH_2Cl)]_{10}$ (**1**).[1] The compound contains a decagon of Fe^{III} centers, each center is thus an isotropic $S = 5/2$, with each edge bridged by two methoxides and one carboxylate. The exchange interactions between the Fe centers is anti-ferromagnetic (AF), leading to an $S = 0$ ground state. Low-temperature magnetization studies show step features as the compound spin ground state changes in the field from $S = 0$, to 1, to 2 and so on. Modeling this magnetic behavior led to the proposal that magnetic molecules could be used to simulate spin waves, previously proposed for extended structures.[1,2]

Such simple and beautiful molecules continue to appeal. For example, beautiful work from Waldmann et al.,[3] has shown that Néel-Vector tunneling of magnetization can be seen in an $\{Fe_{18}\}$ ring prepared by the Christou group. Other studies on the $\{Fe_8\}$ and $\{Fe_{18}\}$ rings has shown that a spin-wave description can be applied to cyclic rings, apparently regardless of the size of the ring.[4]

Chromium(III) rings are as straightforward to make as these iron rings, and are rather more stable. An octanuclear ring, $[CrF(O_2C^tBu)_2]_8$ (**2**) was actually reported slightly before compound **1**,[5] but no detailed magnetic studies were carried out at that time. The compound contains eight equivalent Cr^{III} sites, with each edge bridged by a fluoride and two carboxylates. Later studies reveal the molecule shows equally fascinating physics to **1**, for example, it has step features in magnetization measurements.[6] Cr^{III} is more anisotropic than Fe^{III} and this leads to a richer EPR spectroscopy for **2**.[6] Very recently single-crystal inelastic neutron scattering (INS) studies of **2** have allowed the correlation between the spins to be measured directly, without the need for a spin Hamiltonian.[7] It is the simplicity and elegance of the cyclic structure that allows such studies to be performed.

2. Heterometallic Rings: Synthesis, Variation, and Control of Structure

2.1. Design of a Heterometallic Ring

These cyclic cage complexes led theorists to speculate that new physics would emerge from AF-coupled rings with a spin ground state $\neq 0$.[8] This was an intriguing challenge as up to that point almost all such rings were homometallic and even-numbered. In an even-numbered ring, say **2**, half the metal sites (at the odd-numbered positions) would be spin-up, and

[*] Prof. E. J. L. McInnes, Dr. G. A. Timco, Dr. G. F. S. Whitehead, Prof. R. E. P. Winpenny
School of Chemistry and Photon Science Institute
The University of Manchester
Oxford Road, Manchester M13 9PL (UK)
E-mail: richard.winpenny@manchester.ac.uk

the other half (at the even sites) would be spin-down; the odd- and the even-sub-lattices would cancel completely, and the ground state is always zero.

There seemed two possible routes to produce a magnetic molecule to test these new theories. Firstly, for an odd-numbered homometallic ring it would become impossible to divide the structure into two equal sub-lattices. This situation would create spin frustration and hence the ground state could not be $S=0$ if each spin center had an odd number of electrons, say Fe^{III} or Cr^{III}. Frustratingly, making odd-numbered paramagnetic rings is far from trivial.

Secondly, if a different spin center were introduced into one of the sub-lattices of compound **2** then the two sub-lattices would not cancel perfectly, and the spin ground state would be paramagnetic. After a little thought it became apparent that this could be best achieved in **2** by adding a divalent metal ion that can adopt the same coordination environment as Cr^{III}, and a source of a secondary ammonium cation; both components are needed. Addition of a single divalent ion makes $[Cr_7MF_8(O_2C^tBu)_{16}]^-$ a mono-anion with a central cavity lined with fluoride groups (Figure 1).[9] This cavity is ideal for hosting a cation, such as H_2NR_2, if R is a linear alkyl group, for example, Et or ^{n}Pr. The reaction is then [Eq. (1)]:

$$7\,CrF_3\cdot 4\,H_2O + \text{“}MX_2\text{”} + HNR_2 + \text{xs}\,HO_2C^tBu \rightarrow [H_2NR_2][Cr_7MF_8(O_2C^tBu)_{16}] \quad (1)$$

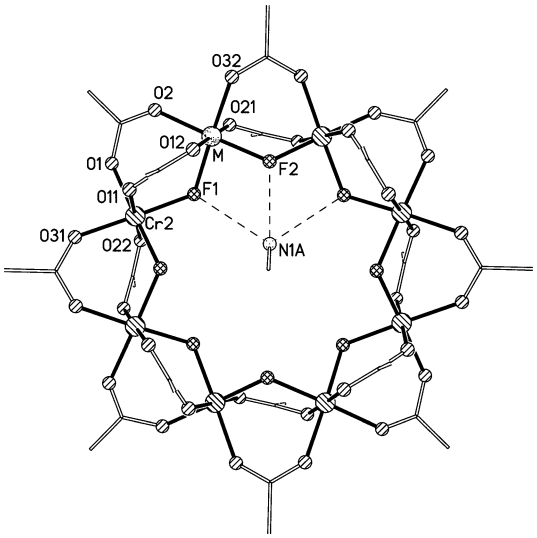

Figure 1. The crystal structure of molecules **3-M**, shown with Me_2NH_2 as the templating cation. H-bonds shown as dotted lines. Shading: Cr, diagonal top left bottom right; other M, dots; F, crossed; O, diagonal top right bottom left; C shown as lines. Me groups of pivalates and H-atoms exclude for clarity.

The resulting compound $[H_2NR_2][Cr_7MF_8(O_2C^tBu)_{16}]$ (**3-M**) can be separated from any **2** formed in the reaction by chromatography. This approach reveals one of the key features of this chemistry—use of Cr^{III} leads to unreactive polymetallic cages. This in turn allows us to develop their chemistry in a manner akin to organic chemistry and use

Eric McInnes has been a Professor of Inorganic Chemistry at The University of Manchester since 2007. He studied at Edinburgh University, and obtained his Ph.D. under the supervision of Prof. Lesley Yellowlees, and undertook post-doctoral positions at Manchester and East Anglia. He is co-Director of the EPSRC National EPR Facility. His research interests are in the chemistry and spectroscopy of the d- and f-block elements, focusing on the magnetic properties of molecule-based materials. In 2015 he was awarded the International EPR Society medal for Chemistry.

George Whitehead his Ph.D. at the University of Manchester in 2013 under the supervision of Prof. Richard Winpenny as part of the North West Nanoscience doctoral training centre focusing on the synthesis, functionalization, and structural characterization of large {Cr_7Ni} heterometallic pseudo-rotaxane assemblies. He was awarded an EPSRC Doctoral Prize and remained at the University of Manchester a further 10 months before starting as a Research Associate in the group of Prof. Matt Rosseinsky at the University of Liverpool in 2014.

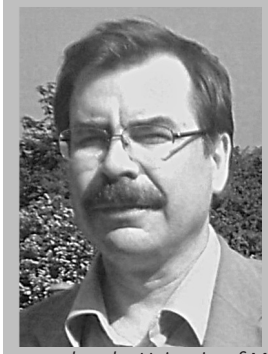

Grigore Timco completed his Ph.D. in 1987 with Prof. Nicolae Gerbeleu at the Institute of Chemistry, Academy of Sciences of Moldova, Chisinau. He was successively Senior Scientific Researcher and Coordinator of Scientific Research in the same institute. He obtained fellowships from the Royal Society to work with Prof. Winpenny, and from the Max-Planck Society and DAAD to pursue research with Prof. Dr. Karl Wieghardt and Dr. Eva Rentschler. The Danish Natural Science Research Council funded research with Prof. Finn Larsen. In May 2003 he moved to the University of Manchester as a senior researcher and since April 2008 has worked as an Honorary Lecturer.

Richard Winpenny studied at Imperial College London and obtained his Ph.D. with Prof. David Goodgame on coordination polymers. After a postdoctoral position with Prof. John Fackler, Jr., at Texas A&M University he joined the staff at the University of Edinburgh. He moved to Manchester as Professor of Inorganic Chemistry in 2000. He won a Royal Society Wolfson Merit Award in 2009 and the Royal Society of Chemistry Tilden Medal in 2011 in recognition of this work.

techniques such as column chromatography. The fact that only one cation can be included in the cavity means charge balance is achieved only for $\{Cr_7M\}$, and not $\{Cr_6M_2\}$. The reaction is therefore remarkably selective, and yields of 80% can be achieved.[9]

Initially the aim was to test the theoretical physics proposals, and so a series of compounds was made varying R and M. It immediately became apparent that any linear alkyl chain could be used as R, but that different compounds result if a branched alkyl chain were used. For M, it seemed sufficient that the divalent metal be able to adopt an octahedral coordination geometry; thus we originally reported $M = Ni^{II}$ (**3-Ni**), Co^{II} (**3-Co**), Fe^{II} (**3-Fe**), Mn^{II} (**3-Mn**), and Zn^{II} (**3-Zn**).[9] Other divalent metals can be included, for example, Mg^{II} and Cd^{II}.[10] Therefore the spin ground state can be controlled in a very systematic way. If we picture adding the divalent metal ion to the odd sub-lattice, this would give the spin of that lattice as $3 \times S_{Cr} + 1 \times S_M$. The even sub-lattice would then have a spin $= 4 \times S_{Cr}$. The ground state S_{GS} must therefore be $|S_{Cr} - S_M|$. So for **3-Ni**, $S_{GS} = 1/2$, for **3-Mn**, $S_{GS} = 1$ and for **3-Zn** $S_{GS} = 3/2$. This can be shown to be correct either from magnetic measurements, or from EPR spectroscopy.[9,11]

The structures of the **3-M** family are clearly related to **2**, with each edge bridged by a fluoride and two carboxylates. One of the carboxylates on each edge lies in the plane of the metal octagon, in an equatorial position, while the second carboxylate lies perpendicular to the metal plane, in an axial position. As we move around the metal octagon, the axial carboxylates are alternately above and below the plane.

Depending on the crystallization solvent used and the secondary ammonium template, the compound crystallizes in tetragonal, orthorhombic, or monoclinic space groups. In some of these space groups there is a four-fold axis passing through the center of the ring, which implies that the divalent metal site is disordered about the ring. The degree of disorder has been studied carefully when the cation is $[H_2NEt_2]^+$ and the compound crystallized from ethyl acetate; this version crystallizes in $P2_1/c$ with a disordered EtOAc in the crystal lattice, and one entire heterometallic ring in the asymmetric unit.[12]

Careful refinement of these structures show that while the heterometal is disordered about the octagon they are not equally distributed about the eight sites of the octagon. As there is an ammonium cation at the center of the ring, hydrogen bonding to the bridging fluorides, there should be a relationship between the positioning of the hydrogen bonds and the location of the divalent metal. Specifically, there will be more electron density on the bridging F^- if it is bound to a divalent metal and hence will more readily form hydrogen bonds. Examining this for **3-M** (M = Ni, Co, Fe, Mn, Cd, Zn) we find that the $[H_2NEt_2]^+$ cation is always disordered over three positions. Matching this with the refined site occupancies of the divalent metal we obtain the picture shown in Figure 2.

In all cases there are three sites (numbers 3, 4, and 7 in Figure 2) in the heterometallic ring at which the divalent metal is not found. For M = Ni, Co, Zn, and Fe, then there is distribution between the five other sites; for the larger

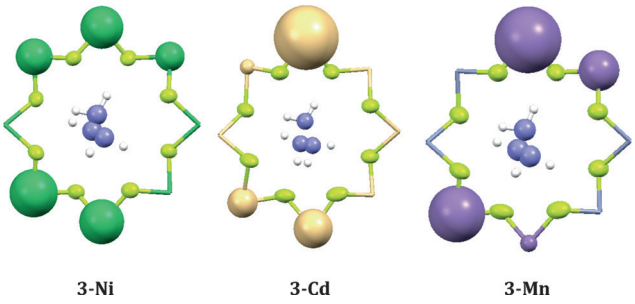

Figure 2. The relative occupancies of M atoms around the ring positions, illustrated with spheres for which the radius indicates the occupancies used in refinement. The sites are numbered in a clockwise fashion, starting at the top center. White H, light blue N, lime green F, green Ni, cream Cd, lilac Mn. Carboxylates excluded for clarity. Taken from Ref. [12] with permission.

divalent ions Cd and Mn, the distribution is more narrow: for **3-Cd** site 1 is 55% Cd, site 5 18% Cd and site 6 10% Cd; for **3-Mn** site 1 is 46% Mn and site 6 33% Mn.[12] Therefore for this combination of cation and crystallization solvent we can say that the crystallographic disorder is incomplete.

Given the ease with which two of the components of the compound can be varied, it seemed advisable to examine how many other components could be varied. The carboxylate used in our first studies was pivalate, but there seemed no reason why other carboxylates shouldn't form this structure. Synthetic studies quickly showed that at least twenty other carboxylates could be included in the octanuclear rings.[13] These ranged from simple variations, for example, *tert*-butylacetate, to carboxylates containing functional groups, such as 3-thiophene carboxylic acid. Some of these carboxylates could be introduced directly by reaction with hydrated chromium trifluoride. Others could be introduced by substitution reactions, that is, firstly making the pivalate version and then heating under reflux for an extended time with the second acid. To date the only carboxylate that we have tried and failed to include in the $\{Cr_7Ni\}$ ring is formate.

As we could vary the divalent metal, it also seemed possible the trivalent metal could be varied. Reactions from the hydrated trifluorides of iron(III), vanadium(III), gallium(III), indium(III), and aluminium(III) all produce $\{M^{III}{}_7M^{II}\}$ rings.[13,14] The Fe^{III} and Group 13 metal rings are unstable with respect to hydrolysis, while the V^{III} rings are also oxygen sensitive. Particularly valuable are the $\{Ga_7Zn\}$ rings as these involve diamagnetic metal ions,[14] and hence give us a diamagnetic host if we wish to study other paramagnetic heterometallic rings without any intermolecular interactions.

2.2. Replacing the Fluoride from Heterometallic Rings

The compounds have the general formula $[H_2NR_2][M_7M'F_8(O_2CR')_{16}]$, where R = Me, Et, ^{n}Pr, ^{n}Bu … ^{n}Oct; M = a trivalent metal; M′ = a divalent ion; O_2CR' = a range of carboxylates. At first it seemed impossible to replace the fluoride in these structures, as fluoride is such a unique ion. We discovered a way to achieve this by adding *N*-ethyl-D-glucamine (H_5Etglu) to the reaction [Eq. (2)].

$$7\,CrF_3\cdot 4\,H_2O + 1/5[2\,MCO_3\cdot 3\,M(OH)_2\cdot 4\,H_2O] + H_5Etglu + xs\,HO_2C^tBu \rightarrow [Cr_7MF_3(Etglu)(O_2C^tBu)_{15}(H_2O)] \quad (2)$$

This reaction produces a compound where the poly-ol is penta-deprotonated, with the five resulting alkoxide groups replacing fluorides to give $[Cr_7MF_3(Etglu)(O_2C^tBu)_{15}(L)]$ **4-M** (Figure 3).[15] As made, the compound contains a mono-

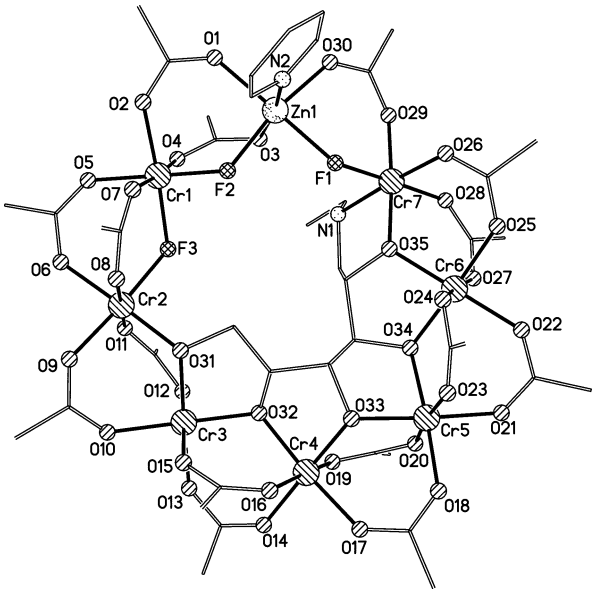

Figure 3. The crystal structure of **4-Zn**, shown with a pyridine ligand attached to the divalent metal site. Shading as Figure 1. Me groups and H-atoms excluded for clarity.

dentate terminal group L = H_2O, but this is easily displaced and for physical studies we have normally used the compounds with L = 4-phenylpyridine.[16] The divalent metal M can be varied, and the compounds with Ni^{II} (**4-Ni**), Mn^{II} (**4-Mn**), Zn^{II} (**4-Zn**), and Co^{II} (**4-Co**) have all been made. If no divalent metal is added we crystallize $[Cr_8F_4(Etglu)(O_2C^tBu)_{15}]$, in which the terminal ligand is fluoride.

The structure of **4** is based around the $Etglu^{5-}$ ligand, which is chiral. The octagon of metal centers is therefore much less regular than in **2** or **3-M**. The internal edges of the octagon are bridged by three fluorides and five alkoxides derived from $Etglu^{5-}$. The divalent site is ordered and bound to two bridging fluorides, three bridging pivalate ligands, and the terminal ligand L. The seven Cr^{III} sites have four distinct coordination environments. One site adjacent to the divalent site metal has an N-donor from $Etglu^{5-}$ coordinated to it, one bridging fluoride, one bridging alkoxide, and three bridging pivalates. The other site adjacent to the M^{II} sites is bound to two μ-fluorides and four oxygen atoms from pivalates. The next Cr site is bound to a single μ-fluoride, a single μ-alkoxide, and four pivalates, while the remaining four Cr^{III} sites are bound to two μ-alkoxides and four pivalates. Five Cr···Cr edges of the ring are bridged by a single alkoxide and two pivalates, the Cr1–Cr2 edge is bridged by a single fluoride and two pivalates, while the two Cr···M edges vary—one bridged by one fluoride and one pivalate the second bridged by one fluoride and two pivalates.

2.3. Variation of the Templating Cation

The addition of an amine to the reaction to give **3-M** or **4-M** is essential; without addition of the amine the major product is always the homometallic $\{Cr_8\}$ ring **2**. As we had originally used secondary amines with linear alkyl groups, it seemed an obvious variation to use branched alkyl groups, for example $(cy\text{-}C_6H_{11})_2NH$ (where $cy\text{-}C_6H_{11}$ is cyclohexyl) in reaction (1), rather than $^nPr_2NH$. This produces a different heterometallic ring, as there is insufficient space within the cavity of an octanuclear ring to include $[H_2N^iPr_2]^+$. Instead compounds form of formulae $[H_2N(cy\text{-}C_6H_{11})_2][Cr_8MF_9(O_2C^tBu)_{18}]$ **5-M**, as shown by elemental analysis and mass spectrometry, however it was not possible with this cation to obtain full crystal data sets for M = Ni or Co.[17] Using $^tBu^iPrNH$ as the secondary amine produces much higher resolution structures for $[H_2N^tBu^iPr][Cr_8MF_9(O_2C^tBu)_{18}]$ **6-M** (M = Ni or Cd) (Figure 4).[18]

The full structures of **6-M** reveal why large odd-metal rings are difficult to form; whereas in **3-M** compounds the axial carboxylates are alternately above and below the plane of the metal octagon, in **6-M** compounds this is impossible—as there are an odd-number of edges. To accommodate the carboxylates the structure has to buckle slightly, and the nine-metal centers are no longer in a single plane (Figure 4b). We

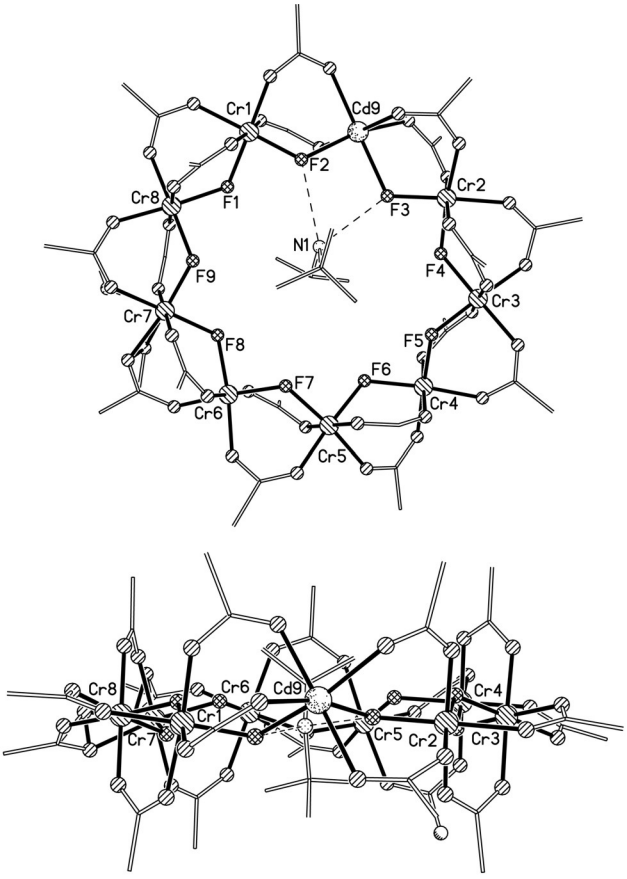

Figure 4. The structure of **6-Cd** shown perpendicular to the mean plane of the metal sites (top) and in the plane of the metals (bottom). Shading as Figure 1. Me groups and H-atoms excluded for clarity.

also find for **6-Cd** that the Cd^{II} site is fully ordered, with the ammonium displaced significantly towards the fluoride ligands bound to the Cd ion.[18] For the reaction that gives **6-Ni** we also find a minor product is a decanuclear ring $[H_2N^tBu^iPr][Cr_9NiF_{10}(O_2C^tBu)_{20}]$ (**7-Ni**).[18] This is a regular planar decagon with one fluoride and two carboxylates on each edge, one in plane with the metal sites of the ring and one either above or below the plane.

This variation in size due to choice of amine suggested many further rings could also be made. The exploration of this area is far from complete as so many different templates could be employed; thus far we have only explored the area with pivalate as the carboxylate. The results for rings with nickel as the divalent metal ion are summarized in Table 1.

As secondary amines work well, it seemed appropriate to also study primary amines, and indeed these can be used to form {Cr_7M} rings, for example, $[^nPrNH_3][Cr_7MF_8(O_2C^tBu)_{16}]$ (**8-M**). The compound where M = Co (**8-Co**) is particularly useful as this allows us to show that the structures are maintained in solution.[19] The fast electron spin relaxation time of the Co^{II} center allows paramagnetically shifted NMR spectra to be recorded on these heterometallic rings. If we compare **3-Co** with **8-Co** we can see the influence of the ammonium cation. For **3-Co** we have a C_2 symmetry axis passing through Co and the Cr *trans* to it in the ring. Therefore there are four unique edges, each with two carboxylates on the edge—one equatorial and one axial. This gives us eight carboxylates in total, and as we are using pivalate we have nine equivalent protons in each carboxylate. As a result we see eight peaks for the carboxylates in the proton NMR spectrum of **3-Co**. For **8-Co** as we have a $[PrNH_3]^+$ cation we remove the C_2 axis, and each edge of the ring is unique, so we now have sixteen carboxylates and see sixteen resonances in the NMR spectrum of **8-Co** (Figure 5).

It would be pleasing to complete the family, and include $[NH_4]^+$ within a ring; this has not been possible to date. We have been able to include other inorganic monocations, such as Cs^+ and Rb^+.[19] They can be made from **8-M** compounds by adding cesium pivalate to the solution, and the primary ammonium is displaced by the alkali-metal cation to give $[Cs][Cr_7MF_8(O_2C^tBu)_{16}]$ (**9-M**). For compound **9-Co** the ^{1}H NMR spectrum indicates we have a C_2 axis, and hence we see eight pivalate resonances (Figure 5); this allows us to follow the conversion of **8-Co** into **9-Co** by ^{1}H NMR spectroscopy, and show that it is fast and quantitative. Rings, such as **3-Co**, templated about secondary ammonium cations, do not exchange with cesium.

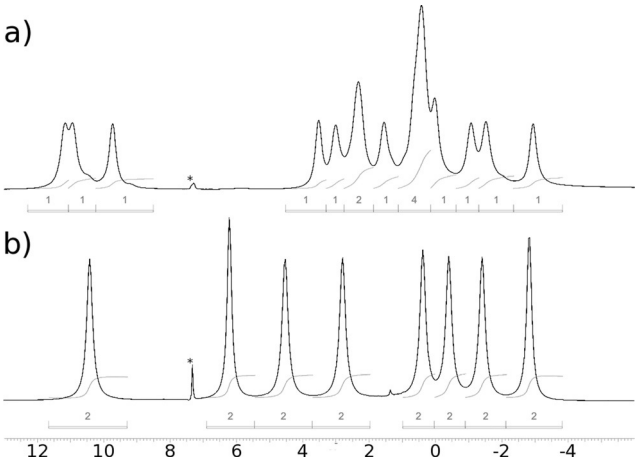

Figure 5. NMR spectra of {Cr_7Co} rings: a) **8-Co** where the primary ammonium template leads to sixteen inequivalent pivalate groups; b) **9-Co**, where a cesium cation produces a twofold axis, and only eight inequivalent pivalates. Taken from Ref. [19] with permission.

Tertiary ammonium cations open up a further group of new rings that has thus far only been explored where Ni^{II} is the divalent ion. Inclusion of $NEt(cy\text{-}C_6H_{11})_2$ in the reaction produces decanuclear rings $[HNEt(cy\text{-}C_6H_{11})_2]$ $[Cr_9NiF_{12}(O_2C^tBu)_{18}]$ (**10-Ni**; Figure 6).[18] These rings are not regular: eight edges contain one fluoride and two carboxylate bridges, while the final two have two fluorides and one carboxylate. These two unusual edges are disposed on opposite sides of the ring. The ammonium template can now only provide one hydrogen atom for H-bonding, and this hydrogen interacts with one of the two fluorides on these edges. The nickel is found disordered over the four sites in the two edges with two F and one pivalate bridge. Using $NMe(cy\text{-}C_6H_{11})_2$ produces a further variant of **10-Ni** but also a compound $[HNMe(cy\text{-}C_6H_{11})_2]_2[Cr_8Ni_2F_{12}(O_2C^tBu)_{18}]$ (**11-Ni**) in which one $[HNMe(cy\text{-}C_6H_{11})_2]^+$ cation is found in the lattice as a counterion, while the second is found inside a $[Cr_8Ni_2F_{12}(O_2C^tBu)_{18}]^{2-}$ dianionic ring; the ring in **11-Ni** is essentially identical to that in **10-Ni**.[18] The two compounds found with the $[HNMe(cy\text{-}C_6H_{11})_2]^+$ can be easily separated by fractional crystallization.

Another group of templates involve substituted imidazolium

Table 1: Cr_xNi_y rings formed by variation of templating cation.

Cation[a]	Code	Formula of ring	Shape	Edge-bridging
NH_2R_2	**3-Ni**	$[Cr_7NiF_8(O_2C^tBu)_{16}]^-$	Regular octagon	8× (1 F, 2 O_2C^tBu)
$NH_2R'_2$	**5-Ni**	$[Cr_8NiF_9(O_2C^tBu)_{18}]^-$	Regular nonagon	9× (1 F, 2 O_2C^tBu)
$H_2N^tBu^iPr$	**6-Ni**	$[Cr_8NiF_9(O_2C^tBu)_{18}]^-$	Regular nonagon	9× (1 F, 2 O_2C^tBu)
$H_2N^tBu^iPr$	**7-Ni**	$[Cr_9NiF_{10}(O_2C^tBu)_{20}]^-$	Regular decagon	10× (1 F, 2 O_2C^tBu)
$^nPrNH_3$	**8-Ni**	$[Cr_7NiF_8(O_2C^tBu)_{16}]^-$	Regular octagon	8× (1 F, 2 O_2C^tBu)
Cs	**9-Ni**	$[Cr_7NiF_8(O_2C^tBu)_{16}]^-$	Regular octagon	8× (1 F, 2 O_2C^tBu)
$HR''(cy\text{-}C_6H_{11})_2N$	**10-Ni**	$[Cr_9NiF_{12}(O_2C^tBu)_{18}]^-$	Irregular decagon	8× (1 F, 2 O_2C^tBu) 2× (2 F, 1 O_2C^tBu)
$HMe(cy\text{-}C_6H_{11})_2N$	**11-Ni**	$[Cr_8Ni_2F_{12}(O_2C^tBu)_{18}]^{2-}$	Irregular decagon	8× (1 F, 2 O_2C^tBu) 2× (2 F, 1 O_2C^tBu)
$(HIm)_2$	**12-Ni**	$[Cr_6Ni_2F_8(O_2C^tBu)_{20}]^{2-}$	Regular octagon	8× (1 F, 2 O_2C^tBu)
$(HIm)_2$	**13-Ni**	$[Cr_8NiF_{11}(O_2C^tBu)_{17}]^{2-}$	Irregular nonagon	8× (1 F, 2 O_2C^tBu) 1× (1 F, 1 O_2C^tBu)
$(HR''Im)_2$	**14-Ni**	$[Cr_8Ni_2F_{12}(O_2C^tBu)_{18}]^{2-}$	Irregular decagon	8× (1 F, 2 O_2C^tBu) 2× (2 F, 1 O_2C^tBu)
$(HBzIm)_2$	**15-Ni**	$[Cr_7Ni_2F_9(O_2C^tBu)_{18}]^{2-}$	Regular nonagon	9× (1 F, 2 O_2C^tBu)
$[Ni(tacn)_2]^{2+}$	**16-Ni**	$[Cr_8Ni_2F_{10}(O_2C^tBu)_{20}]^{2-}$	Regular decagon	10× (1 F, 2 O_2C^tBu)

[a] R = linear alkyl; R′ = *cy*-C_6H_{11}; R″ = Me or Et; Him = imidazolium; BzIm = 1-benzylimidazolium.

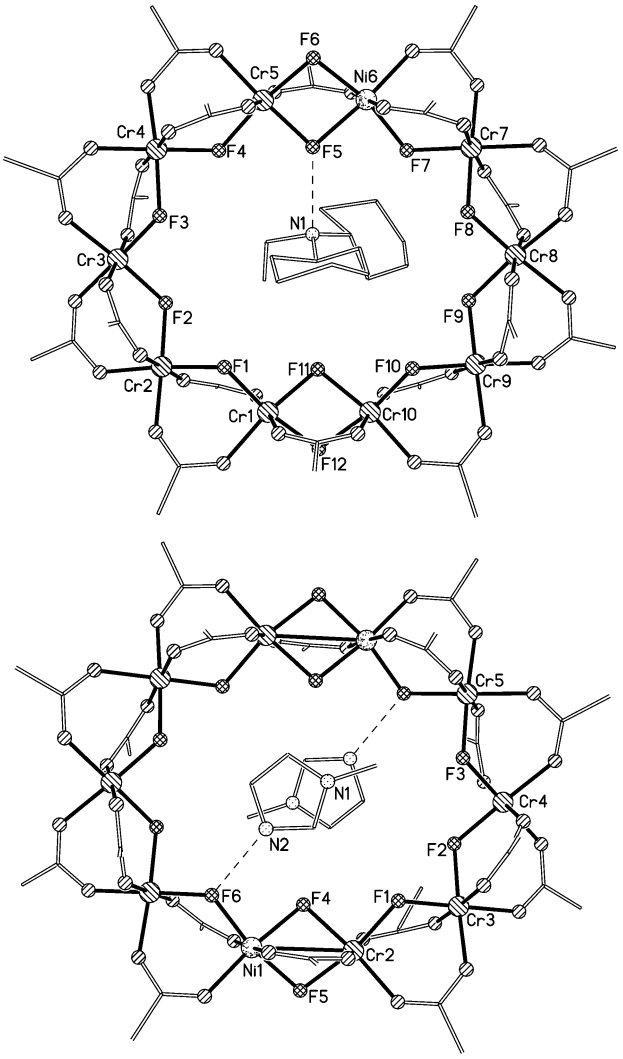

Figure 6. The structures of two decametallic rings. Top: **10-Ni**; bottom: **14-Ni**. In **14-Ni** there are two Ni sites in the ring, and two isomers are possible, the centrosymmetric isomer is shown. Shading as Figure 1. H-atoms and Me groups excluded for clarity.

cations.[18] With 2,4-dimethylimidazole a further version of structure **3** results, with an imidazolium cation. With other imidazoles more complicated structures result. With imidazole itself two compounds are found: $[HIm]_2[Cr_6Ni_2F_8(O_2C^tBu)_{20}]$ (**12-Ni**; where HIm = imidazolium), with both cations found inside the ring, stacking on top of one another with the centroid of one N-heterocycle 3.35 Å above the other.[18] The dianionic $[Cr_6Ni_2F_8(O_2C^tBu)_{20}]^{2-}$ is structurally identical to the monoanionic rings found in **3-Ni**, **8-Ni**, and **9-Ni**. The second product of this reaction is $[HIm]_2[Cr_8NiF_{11}(O_2C^tBu)_{17}]$ (**13-Ni**), which contains a nonagon of metals, but where one edge is bridged by a single fluoride and a single pivalate, with two terminal fluorides found on the metals on this edge. The Ni is delocalized on this edge.

The imidazole used can be substituted, for example, using *N*-methyl or *N*-*n*-butyl-imidazole produces irregular decanuclear rings related to those found in **10-Ni** and **11-Ni**; $[HR''Im]_2[Cr_8Ni_2F_{12}(O_2C^tBu)_{18}]$ (**14-Ni**; R″ = Me or ^{n}Bu) contain two imidazolium cations, again with a stacking interaction between the N-heterocycles (Figure 6). These rings containing two divalent ions have the possibility of isomers depending on the separation of the metal sites.[18]

With 1-benzylimidazole (BzIm) a nonanuclear ring is formed: $[BzImH]_2[Cr_7Ni_2F_9(O_2C^tBu)_{18}]$ (**15-Ni**), which is a regular ring with each edge bridged by two pivalates and a fluoride, but with two Ni sites disordered around the ring.[18] The presence of linkage isomers in **15-Ni** and **12-Ni** has been investigated by EPR spectroscopy and magnetic studies.[20] In **12-Ni** at least two isomers are found, one in which both nickel sites are in the same sub-lattice (i.e. Ni at odd-numbered positions around the ring) and one in which the nickel sites are in different sub-lattices (e.g. adjacent in the ring). Compound **15-Ni** has an $S = 1/2$ ground state—as would be expected for any frustrated nine-metal ring with an odd number of electrons—and there is no strong evidence for more than one isomer being present.

One final variation in the template we have explored is to use a metal complex. Complexes of 1,4,7-triazacyclononane (H_3tacn) work well, and compounds, such as $[M'(tacn)_2][Cr_8M_2F_{10}(O_2C^tBu)_{20}]$ (**16-MM′**) can be crystallized (Figure 7).[21] Thus far only **16-NiNi** has been reported, but there is no reason that the family cannot be extended. As the $[Ni(tacn)_2]^{2+}$ unit is a large dication, the heterometallic ring expands to a regular decagon, and it has to include two divalent metal sites to charge balance. The low-temperature magnetic susceptibility is equivalent to that of an isolated Ni^{II} ion; this is presumably due to the $[Ni(tacn)_2]^{2+}$ template which implies that the $\{Cr_8Ni_2\}$ ring has an $S = 0$ spin ground state. In turn this must mean that the two Ni^{II} ions neighbor each other in the structure as one must belong to the odd sub-lattice and the other to the even.

Seeking to make even larger rings a complex of cyclen (1,4,7,10-tetrazacyclododecane) was used; this does not produce a ring but sometimes there is no success like failure.

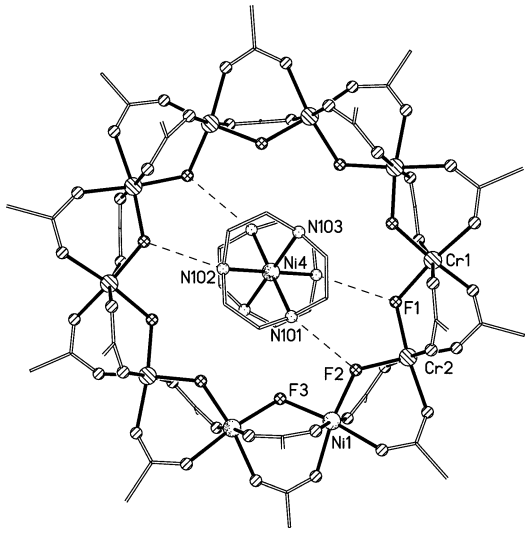

Figure 7. The crystal structure of **16-NiNi**. The two Ni sites in the metal ring are presumed to be next to one another based on magnetic data that suggest an $S = 0$ ground state for the $\{Cr_8Ni_2\}$ ring. Shading as Figure 1. H-atoms and Me groups excluded for clarity.

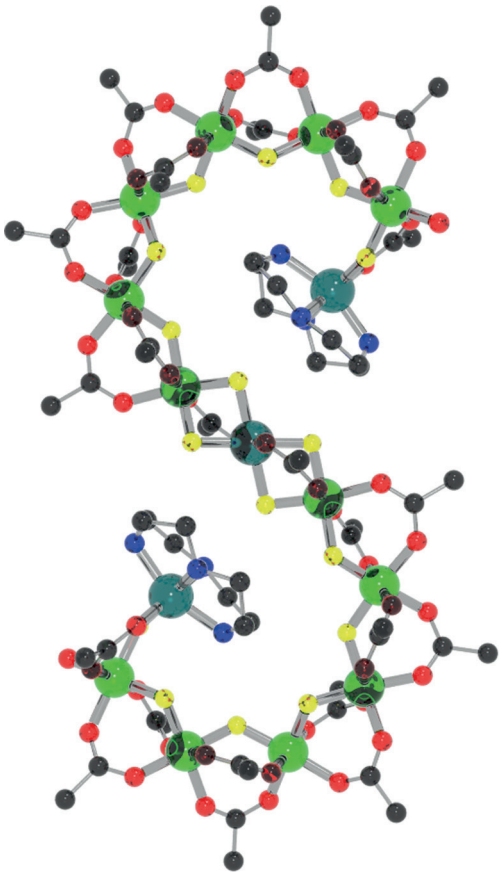

Figure 8. The crystal structure of **17-NiNi**. Cr light green; Ni dark green; F yellow; O red; N blue; C black. H-atoms and Me groups excluded for clarity.

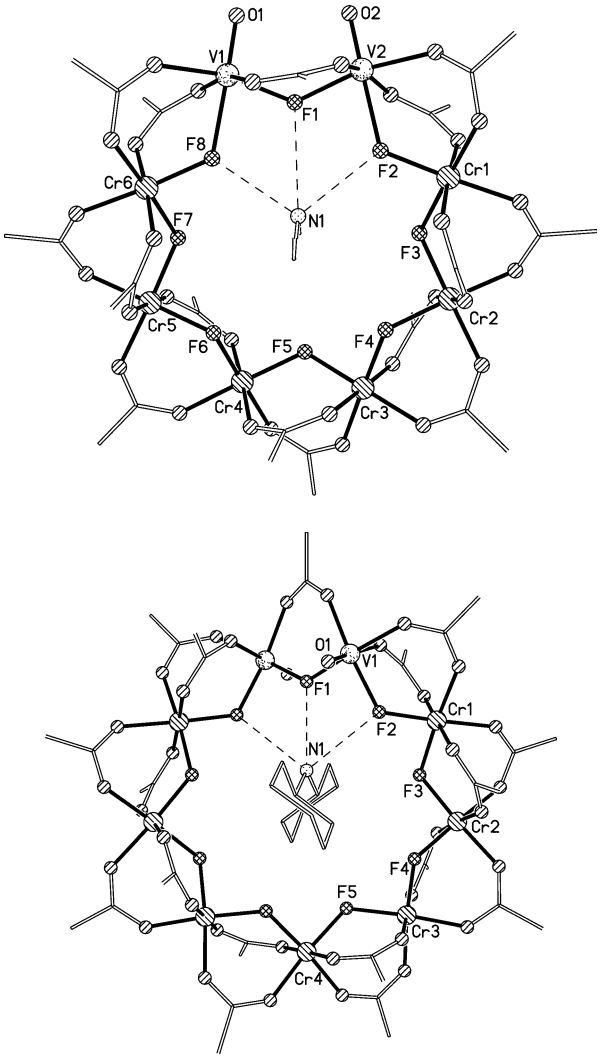

Figure 9. The structures of $\{Cr_x(VO)_2\}$ rings. Top: **18**. Bottom: **19**. Shading as Figure 1. H-atoms and Me groups excluded for clarity.

Instead, an S-shaped molecule crystallizes of formula $[Ni(cyclen)_2Cr_{12}NiF_{20}(O_2C^tBu)_{22}]$ (**17-NiNi**; Figure 8).[21] The two Ni(cyclen) units are found at the termini of the molecule, with the additional Ni^{II} at the center of the S. The two cyclens bind leaving *cis*-sites vacant on the Ni sites, and these sites are occupied by a bridging pivalate and a μ_2-fluoride. The Cr···Cr contacts are each bridged by a fluoride and two carboxylates, while the two central Cr···Ni contacts are bridged by two fluorides and a carboxylate in a similar manner to that found in the irregular decanuclear rings **10-Ni**, **11-Ni**, and **14-Ni**.

2.4. Dicationic Ions and Irregular Divalent Ions

Divalent metals that will adopt octahedral coordination geometries form compounds **3-M** readily. It therefore seemed worth exploring what happens with 3d metals that do not readily fit into octahedral holes. Using VO^{2+} in place of the divalent metal we make compounds that include two vanadyls in the ring, and again we can control the ring size by the choice of template.[17,22] Thus with secondary ammonium cations with linear alkyl chains we find $[H_2NR_2][Cr_6(VO)_2F_8(O_2C^tBu)_{15}]$ (**18**; e.g. R = Et)[22] and with branched chains we find $[H_2NR'_2][Cr_7(VO)_2F_9(O_2C^tBu)_{17}]$ (**19**; e.g. R′ = cyclohexyl; Figure 9).[17] Initially these structures appear completely ordered, with the two vanadyl units next to one another and the V···V edge bridged by a single fluoride and a single carboxylate; the Cr···V and Cr···Cr edges are bridged as in **3-M** compounds. The ammonium cation lies at the center of the cavity and is H-bonded to fluorides bound to vanadyl. However careful chromatography and crystallography reveals that this chemistry is slightly more complicated. A $(CrF)^{2+}$ unit has the same charge and a very similar size to the $(VO)^{2+}$ unit, and so the compounds as originally crystallized also contain some $[H_2NR_2][Cr_6(CrF)(VO)F_8(O_2C^tBu)_{15}]$ or $[H_2NR'_2][Cr_7(CrF)(VO)F_9(O_2C^tBu)_{17}]$.

Inclusion of Cu^{II} in this chemistry brings a new series of compounds, and reveals a more complicated chemistry than found for other metals.[22–25] The compound $[NH_2Et_2][Cr_7CuF_8(O_2C^tBu)_{16}]$ **3-Cu** can be made from a pre-formed $\{Cr_7\}$ horseshoe (see below).[25] The crystallographic studies of this compound suggest the copper ion is occupying a regular octahedral coordination site, but detailed EPR and INS studies show that there is a Jahn–Teller distortion of the electronic structure; this is confirmed by a DFT calculation,

which shows that the energy of the compound is reduced if there is an elongation of one Cu–F bond, and the Cu–O bond *trans* to it.

If reaction (1) is performed with basic copper carbonate the structure again depends on the secondary amine involved and also on the reaction time. If $^{i}Pr_2NH$ is used and the reaction heated for 5 h, $[H_2N^{i}Pr_2]_2[Cr_{10}Cu_2F_{14}(O_2C^{t}Bu)_{22}]$ (**20**) results (Figure 10).[23] Heating the reaction for a day gives two

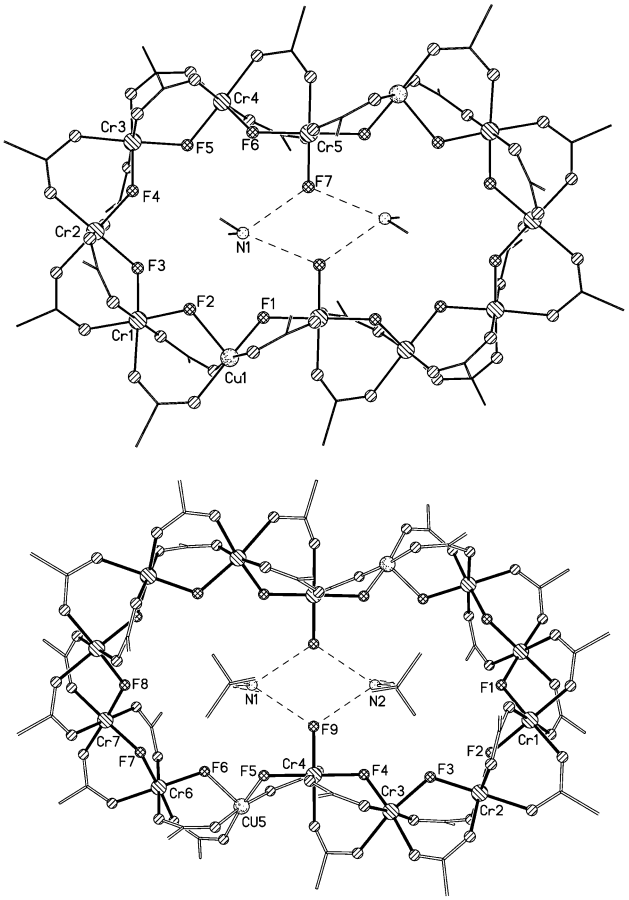

Figure 10. The structure of $\{Cr_xCu_2\}$ rings. Top: **20**. Bottom: **21**. Shading as Figure 1. H-atoms and Me groups excluded for clarity.

products: a major product $[H_2N^{i}Pr_2]_2[Cr_{12}Cu_2F_{16}(O_2C^{t}Bu)_{26}]$ (**21**) and a minor product $[H_2N^{i}Pr_2]_2[Cr_{11}Cu_2F_{15}(O_2C^{t}Bu)_{24}]$ (**22**); these compounds are very clearly related with a general formula $[H_2N^{i}Pr_2]_2[Cr_xCu_2F_{x+4}(O_2C^{t}Bu)_{2x+2}]$.[24] All contain two five-coordinate Cu^{II} sites linked by Cr chains that contain five Cr^{III} centers in **20**, six Cr^{III} centers in **21**, and a mixture in **22**. As in all the compounds discussed to this point the Cr···Cr edges are bridged by a fluoride and two carboxylates. One Cr···Cu edge is similarly bridged, while the other is bridged by a fluoride and a single carboxylate. One Cr site therefore has to have a terminal fluoride group attached to it to make it six coordinate. The two ammonium cations are found at the center of the cyclic molecule, which resembles an hour-glass rather than a ring in each case.

Use of benzimidazole (Bz) produces a further cyclic molecule: $[HBz]_2[Cr_8Cu_2F_{14}(O_2C\mathit{t}Bu)_{16}(Bz)_2]$ (**23**).[24] In this case the Cu^{II} sites are linked by $\{Cr_4\}$ chains, with the usual bridges in place on the Cr···Cr edges. The four Cr···Cu edges are each bridged by a fluoride and a carboxylate, leaving terminal fluorides on all the Cr sites adjacent to the Cu sites. These terminal fluorides H-bond to the HBz cations, but these are exterior to the ring in **23**, unlike all our previous cyclic compounds. Two neutral Bz ligands are found in the cavity of the ring, each bound through an N-donor to a copper site. This chemistry involving copper(II) is therefore possibly even richer than that involving nickel(II).

2.5. Horseshoe Structures and Complexes of Horseshoes

The wealth of chemistry that arises from simple variations of one reaction led us to examine removing one component from it, namely the source of a divalent metal. This change produces a new family of chromium complexes that can themselves then be used as reactants to produce new heterometallic complexes. It is noticeable that even without the divalent metal the addition of an amine to the reaction is sufficient to prevent the formation of compound **2**.

These compounds resemble horseshoes, and contain between three and seven chromium centers. The first made involved using $^{n}Pr_2NH$ as the amine and has the formula $[(H_2N^{n}Pr_2)_3\{Cr_6F_{11}(O_2C^{t}Bu)_{10}(H_2O)_2\}_2]$ (**24**; Figure 11);[22] other variants of this structural type can be made with other secondary ammonium cations with linear alkyl chains, such as $[H_2NEt_2]^+$ and $[H_2N^{n}Bu_2]^+$. The same $\{Cr_6\}$ horseshoe is found when $[H_2NMe_2]^+$ is the cation, however in this case a tetramer of horseshoes is formed: $[(H_2NMe_2)_3\{Cr_6F_{11}(O_2C^{t}Bu)_{10}(H_2O)_{2.5}\}_4]$ (**25**).[26] The compounds share the common features that the Cr···Cr contacts within the horseshoes are all bridged by one fluoride and two carboxylates, with the coordinate sites of the terminal Cr sites each occupied by three terminal fluorides. These fluorides H-bond to the ammonium cations, leading to supramolecular dimers or tetramers; it is presumably the smaller steric requirements of methyl groups that allows the tetramer **25** to form in preference to the dimers.

Changing the secondary amine produces other horseshoes. With $[H_2N^{i}Pr_2]^+$ as the cation $[(H_2N^{i}Pr_2)_3\{Cr_7F_{12}(O_2C^{t}Bu)_{12}(H_2O)_2\}_2]$ (**26**), forms which is simply a slightly larger version of **24**. A $\{Cr_3\}$ horseshoe can be formed with di-*n*-octylamine: $[(H_2N^{n}Oct_2)_3\{Cr_3F_8(O_2C^{t}Bu)_4(HO_2C^{t}Bu)_2\}]_n$ (**27**), which forms a one-dimensional H-bonded polymer in the crystal.[27] Compounds **24**–**27** are therefore clearly part of a family of horseshoes with the chromium fragments having the general formula $[Cr_xF_{x+5}(O_2C^{t}Bu)_{2x-2}(sol)_y]$. Looking again at the cyclic structures we can find these horseshoes as components of the rings, and it was the isolation of **26** and its onward reaction with copper carbonate that allowed us to make **3-Cu**. Examining these structures shows that while the $\{Cr_4\}$, $\{Cr_5\}$, and $\{Cr_8\}$ horseshoes have not yet been produced in isolation they are found, for example, in compounds **23**, **20**, and **5** respectively.

The presence of terminal fluoride groups suggests that perhaps the horseshoes could either react with other ligands,

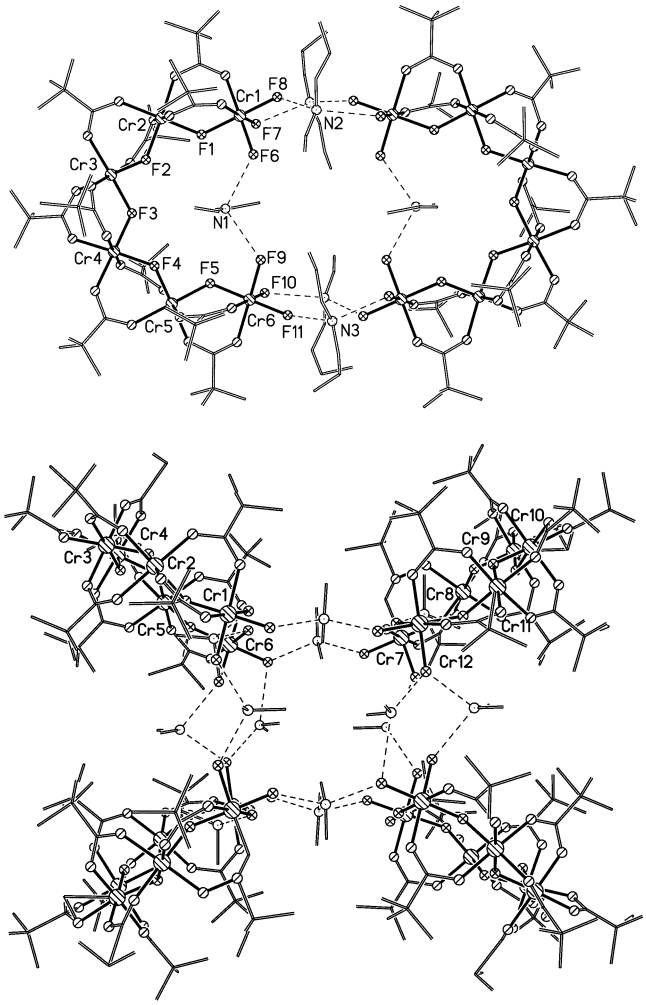

Figure 11. The structures of assemblies of $\{Cr_6\}$ horseshoes. Top: **24**. Bottom: **25**. Shading as Figure 1. H-atoms and Me groups excluded for clarity.

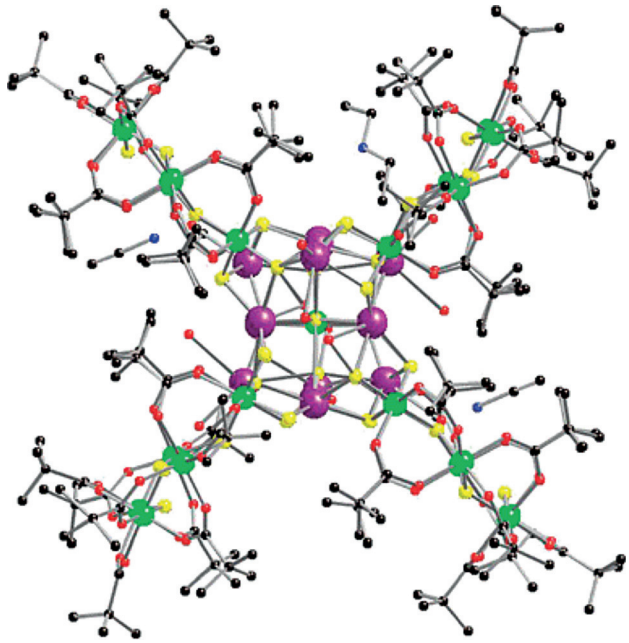

Figure 12. The crystal structure of **30**. Colors as Figure 8, plus Na purple. H-atoms excluded for clarity.

or act as ligands for fluorophilic metal ions. Reaction of **23** or **24** with a β-diketonate or a salt of such a ligand displaces two of the terminal fluorides on each terminal Cr^{III} ion, giving $[(H_2NEt_2)\{Cr_6F_7(O_2C^tBu)_{10}(hfac)_2\}]$ (**28**) or $[(H_2N^iPr_2)\{Cr_7F_8(O_2C^tBu)_{12}(hfac)_2\}]$ (**29**), respectively (Hhfac = 1,1,1,5,5,5-hexafluoroacetylacetonate).[28] This approach allows us to study the physical behavior of the isolated horseshoes. A single ammonium cation is retained at the center of each horseshoe.

Reaction with s- or f-block metal complexes is more interesting.[27] Reaction of **24** with sodium azide or sodium isocyanate gives $[\{CrNa_{14}F_6(H_2O)_{10}\}(H_2NEt_2)\{Cr_6F_{11}(O_2C^tBu)_{12}\}_4]$ (**30**; Figure 12). This compound contains four $\{Cr_6\}$ horseshoes, with no ammonium at the center of the horseshoe. The fluorides coordinate to an unusual $\{CrNa_{14}\}$ cage. At the center of this cage is a CrF_6 unit, surrounded by an icosahedron of twelve Na^+ ions; two further sodium ions are attached to the cage through bridging fluorides.

Reactions with lanthanide pivalate complexes give a range of compounds that seem sensitive to the size of the lanthanide ion.[29] Reaction of **24** with cerium pivalate gives $[Cr_6CeF_7(O_2C^tBu)_{14}(THF)_2]$ (**31**; Figure 13); this is only the second heptanuclear ring reported[30] and the structure is clearly related to the octa-, nona-, and decanuclear rings described above. A fluoride and two carboxylates bridge each edge of the structure. The cerium site is eight-coordinate, bound to two THF molecules, derived from the recrystallization solvent. We have been unable to make equivalent structures with smaller lanthanides.

Reaction of **24** with gadolinium pivalate gives a metal bicycle: $[\{(H_2NEt_2)(Cr_6GdF_9(O_2C^tBu)_{13}\}_2]$ (**32**; Figure 13).[29] This species can either be described as two $\{Cr_6Gd_2\}$ rings sharing the Gd···Gd edge, or regarded as two $\{Cr_6\}$ horseshoes acting as ligands for a $\{Gd_2\}$ dimer. The Cr coordination and bridging within the $\{Cr_6\}$ is exactly as we have seen before. The Gd sites are eight coordinate, with the central Gd···Gd contact bridged by two pivalates, and the Cr···Gd contacts each bridged by two fluorides and a pivalate.

This compound is not the most easily made product. Heating the reaction that gives **32** leads to a related cage: $[(Gd_4F_7(O_2C^tBu))\{(H_2NEt_2)(Cr_6F_7(O_2C^tBu)_{14}\}_2]$ (**33-Gd**; Figure 13). This compound is best described as two $\{Cr_6\}$ horseshoes acting as ligands to a central $\{Gd_4F_7\}$ cage, which has some analogies to the structure of **30**. Each Gd^{III} site in **33-Gd** is eight coordinate, to two O-donors from pivalate and six bridging fluorides. The two $\{Cr_6\}$ horseshoes are almost orthogonal to one another about the central unit, unlike in **32** where they are co-planar. Compounds isostructural to **33** can be made with lanthanides heavier than gadolinium and with yttrium, **33-Y**. The reaction with yttrium introduces an additional member of this family, an octanuclear wheel $[(H_2NEt_2)\{Cr_6Y_2F_8(O_2C^tBu)_{17}(H_2O)]$ (**34**).[29] In this case the Cr···Cr and Cr···Y edges are bridged by one fluoride and two pivalates, while the Y···Y edge is bridged by one fluoride and three carboxylates. The Y^{III} sites are both eight coordinate.

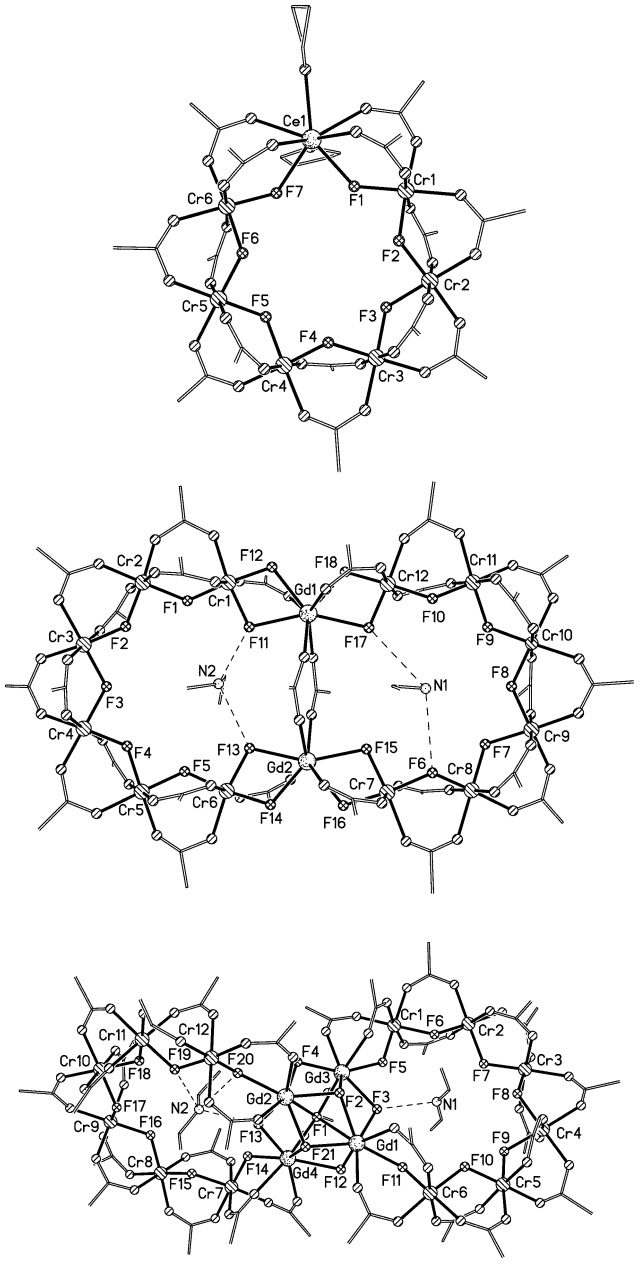

Figure 13. The structures of lanthanide complexes of $\{Cr_6\}$ horseshoes. Top: **31**. Middle: **32**. Bottom: **33**. Shading as Figure 1. H-atoms and Me groups excluded for clarity.

These structures with yttrium are the first with Group 3 of the periodic table, and heterometallic rings involving chromium have now been structurally characterized for members of every group up to Group 13, with the exception of Group 4 (see Scheme 1), and with the 4f ions. The only metallic elements not thus far included in this family are the 5d or 5f metals, and the metalloids in Group 14 and 15.

3. Physical Studies of Single Heterometallic Rings

The synthetic control possible with the heterometallic rings, and the range of resulting compounds creates the possibility of a systematic study of the magnetic properties of a vast family of compounds. Even more fortunately, these compounds give quite remarkably clear spectra, both for electron paramagnetic resonance (EPR) spectroscopy and for inelastic neutron scattering (INS) spectroscopy. Finally, large single crystals can be grown—the largest weighing over 4 grams. Taken together, these properties create an unprecedented opportunity.

3.1. Magnetic Studies and INS Spectroscopy of {Cr$_7$M} Rings

Magnetic studies of the many members of the **3-M** and **4-M** families show very similar behavior.[9,16,20,31] The large number of experiments performed has led to a large number of Hamiltonians being used; herein we have standardized all these results, and all are reported for a Hamiltonian where the exchange interaction is of the form $\hat{H} = -2JS_1S_2$, which means that ferromagnetic interactions have a positive sign and antiferromagnetic interactions are negative. With the exception of **3-Cu**[25] all the exchange interactions between nearest neighbors are antiferromagnetic, and produce a ground state that is predictable from the simple alternation of spins up and down. For **3-Ni** and **4-Ni** this gives a ground state of $S_{GS} = 1/2$; for **3-Mn** and **4-Mn** this gives $S_{GS} = 1$ and for **3-Zn**, **3-Cd**, and **4-Zn** $S_{GS} = 3/2$.[9,16] The magnetic data can be fitted to derive exchange interactions, but these exchange interactions can be better derived from INS spectroscopy.[32] The spin Hamiltonian parameters, measured by INS studies as well as magnetic measurements, are given in Table 2.

Compound **3-Fe** has also been studied by variable-temperature susceptibility and low-temperature magnetization measurements only, and has an $S = 1/2$ ground state.[31] The fit of this data is somewhat different, using only one exchange interaction for both the J_{CrCr} and J_{FeCr} interactions; this exchange interaction is reported to be $-4.45\ cm^{-1}$; in all other **3-M** compounds, J_{CrCr} is consistent, and larger at $-5.9\ cm^{-1}$. This would suggest that J_{CrFe} should be much smaller than $-4.45\ cm^{-1}$ to account for the magnetic behavior. No INS data have been recorded on this compound.

1	*2*	*3*	*4*	*5*	*6*	*7*	*8*	*9*	*10*	*11*	*12*	*13*
Na	*Mg*											*Al*
30	3											3
K	*Ca*	*Sc*	*Ti*	*V*	*Cr*	*Mn*	*Fe*	*Co*	*Ni*	*Cu*	*Zn*	*Ga*
	3			18, 19	ALL	3, 4	3, 4	3, 4, 8, 9	3, 4 – 17	3, 20-23	3, 4	3
Rb	*Sr*	*Y*									*Cd*	*In*
9	3	34									3, 4, 6	3
Cs	*Ba*	*La-Lu*										
9	3	31-33										

Scheme 1. A periodic table of ring structural types.

Table 2: Spin Hamiltonian parameters for **3-M** and **4-M** compounds.

Cmpd.	J_{CrCr} [cm^{-1}]	J_{CrM} [cm^{-1}]	d_{Cr}[a] [cm^{-1}]	d_{M}[a] [cm^{-1}]	Ref.
3-Ni	−5.87	−6.81	−0.16	−1.6	[32]
3-Zn	−5.87	–	−0.16		[32]
3-Mn	−5.87	−5.53	−0.16	−0.05	[32]
3-Cu	−5.91	−11.99, +6.50	−0.14	–	[25]
3-Fe	−4.45	−4.45	n.r.[b]	n.r.[b]	[31]
4-Zn	−6.95	–	−0.12	–	[16]
4-Mn	−6.95	−4.17	−0.12	−0.01	[16]
4-Ni	−6.95	−10.43	−0.12	−2.54	[16]

[a] Single ion axial anisotropy parameter derived from INS and EPR spectroscopy. [b] Not reported.

For **3-Cu** the value of INS measurements is very clear.[25] The thermodynamic measurements alone can be fitted with J_{CrCr} and a single J_{CrCu} resulting in an $S=1$ ground state. However, the INS measurements show a low-energy peak that can only be a transition from this state to a very low-lying $S=0$ state (Figure 14). Such a state can only arise if there is one very small exchange interaction or a ferromagnetic exchange interaction. Therefore to fit the magnetic and INS data simultaneously a model with $J_{CrCr}=-5.9\ cm^{-1}$ and two $J_{CrCu,}$ with values of −12.0 and +6.5 cm^{-1} is used. The need for two different exchange interactions comes from the very anisotropic electronic structure of the Jahn–Teller distorted d^9 ion.[25] This distortion is not seen in the X-ray crystal structure, where no pair of *trans* bonds is observed as elongated, but it is seen by DFT calculations; if the structure is minimized, a low energy form is found with one Cu–F bond and the Cu–O bond *trans* to it elongated.

Given this observation it is surprising that in the **4-M** family all thermodynamic data, both magnetic and specific heat measurements, and INS spectra measured on a family member can be fitted with one J_{CrCr} and one J_{CrM}.[16] The results are tabulated in Table 2. This is despite the considerable variation in the two Cr···M edges in the structure. We have not yet made and studied **4-Cu** or **4-Fe** and perhaps these would show a significant variation.

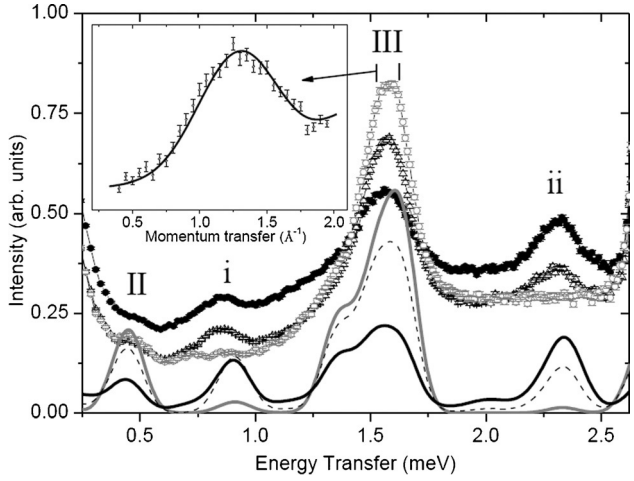

Figure 14. INS energy spectra at 5.0 Å of **3-Cu**, measured at 1.93 K (gray open circles), 6.0 K (black open triangles) and 15.0 K (black circles). The solid lines show theoretical simulated results at 1.93 K (gray), 6 K (black broken line) and 15 K (black), using parameters given in Table 2. Insert shows the Q dependence for the 1.57 meV transition (**III**), measured at 1.93 K, where the solid line represents the calculated Q dependence. Taken from Ref. [25] with permission.

These studies feed into more advanced studies on specific examples of the family investigating how the symmetry of the heterometallic rings influences spin dynamics when compared with the homometallic rings. The $\{Cr_8\}$ ring **2** has approximately D_{4d} point symmetry while a heterometallic ring, for example **3-M**, has at best C_2 symmetry. This symmetry has important consequences for whether energy levels of the system can mix or cross in varying magnetic field.

For **2** a low-temperature study of the torque magnetometry shows step features as the field increases.[33] This is because while the ground state is $S=0$ in zero-field, as the field increases the microstates within the first excited $S=1$ state, split, with $|1, -1\rangle$ falling in energy (where the energy level is labeled as $|S, m_S\rangle$) due to the Zeeman effect. Similarly the $S=2$ second excited states splits, with the $|2, -2\rangle$ falling in energy, twice as fast as the $|1, -1\rangle$ falls, and so on for $S=3$, $S=4$, and higher spin states. The result is that at specific critical fields the lowest energy state changes, firstly from $|0, 0\rangle$ to $|1, -1\rangle$ then $|2, -2\rangle$ then $|3, -3\rangle$.[33] As **2** has very high symmetry these different states belong to different irreducible representations, which means they are allowed to cross and there are sharp step transitions at each critical field.

For **3-M** compounds (studied for M = Ni, Zn, and Mn), the spin levels split in an analogous way, but the symmetry of the molecule is much lower, and hence the individual spin states belong to the same irreducible representation.[34] Thus for **3-Ni** the ground state is initially $|1/2, -1/2\rangle$ and then becomes $|3/2, -3/2\rangle$, and then $|5/2, -5/2\rangle$. However, now at the critical fields, the states can mix, and the crossings become avoided crossings. This mixing leads to a fluctuation of the total spin of the system at the avoided crossings, and this is seen in the torque magnetometry as peaks in the response with field (Figure 15).[34]

The ability to grow large crystals, weighing 4 grams or more, of this family of compounds allows an even more elegant experiment. Single-crystal INS spectra of **3-Ni** have been recorded at low temperature, and to 11.5 T external magnetic field.[35] By orienting the external field with respect to the perpendicular axis of the molecule we can maximize the mixing of the states, for example, $|1/2, -1/2\rangle$, and $|3/2, -3/2\rangle$, and then study the behavior at the avoided crossing. The calculation predicts that the two states curve to avoid crossing, and we can see this by monitoring the INS transition between the states as a function of field.[35] This transition falls in energy as the $|3/2, -3/2\rangle$ state falls in energy, but the transition energy becomes constant as we reach the avoided crossing and we can then measure the avoided-crossing energy precisely using the INS spectroscopy (Figure 16). Such an experiment had not previously been performed for molecular species.

Magnetic and INS studies of larger rings are not so advanced. Studies of **5-Ni** have been performed,[17] and give $J_{CrCr}=-5.28$, $J_{CrNi}=-12.99\ cm^{-1}$. This gives an $S=0$ ground

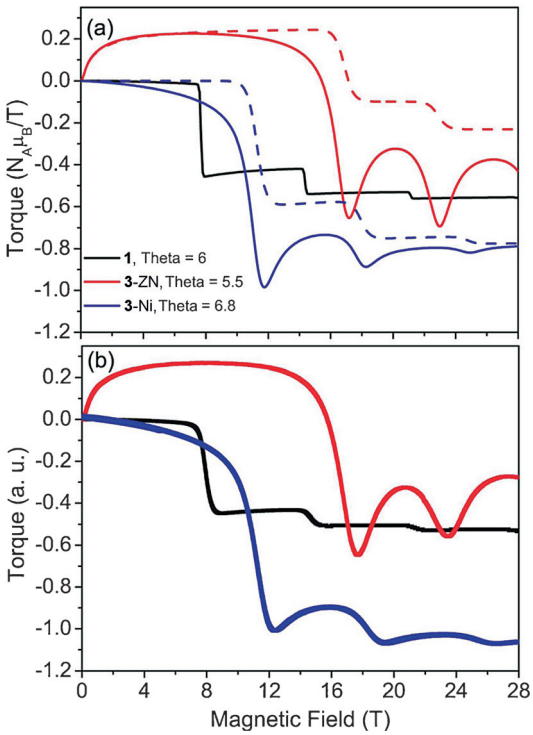

Figure 15. a) Solid lines: calculated torque versus the applied field intensity *B* for **1** ($T = 50$ mK), **3-Zn** and **3-Ni** ($T = 400$ mK). Dashed lines: the same for **3-Zn** and **3-Ni** with *S*-mixing forced to zero. b) Experimental results for the same conditions as in (a). Taken from Ref. [33] with permission.

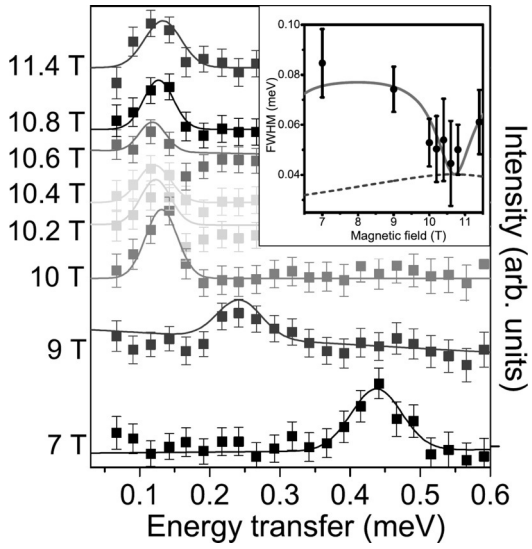

Figure 16. High-resolution INS data ($\lambda = 7$ Å) for $\{Cr_7Ni\}$ at $T = 66$ mK for different applied field at 50° to the ring axis, *z*. Data are offset vertically for clarity and background corrections have been applied. The lines represent fits to the sum of a Gaussian and a sloping background. The inset shows the field dependence of the width of the peaks. The line is the full width at half maximum (FWHM) of the convolution of the instrument resolution function and a Gaussian of standard deviation $\sigma = \sigma_J \delta\Delta_{AC}/\delta J$, where $\sigma = 0.025$ J. The dashed line shows the instrument resolution. Taken from Ref. [35] with permission.

state for the nonanuclear ring, a spin state that cannot be derived from the classical picture of spins. This has led to **5-Ni** being described as a magnetic Möbius strip,[17a] in which the spin structure is not alternately "up and down" around the ring. INS studies of **5-Zn** give a very similar value for J_{CrCr}.[17c]

Very recently polarized neutron diffraction (PND) studies have been reported for a further nonanuclear ring, **6-Cd**;[17d] this allows the spin density at each metal site to be measured directly. The PND measurements were performed with applied magnetic fields of 4.6 and 9 T, and at a temperature of 1.8 K. While **6-Cd** has an $S = 0$ ground state in zero external field, at 4.6 T the ground state is $S = 1$, and at 9 T, the ground state is $S = 2$. The spin in these states is not delocalized equally over the eight Cr sites of the $\{Cr_8Cd\}$ ring. The two Cr sites adjacent to Cd (Cr1 and Cr8, numbering around the ring) have by the far the largest share of the spin (0.93 μ_B at 4.6 T and 1.59 μ_B at 9 T).[17d] Moving to the next Cr sites in the chain (Cr2 and Cr7), the spin density is found to be of the opposite sign due to the antiferromagnetic exchange, and much lower (average −0.31 μ_B at 4.6 T, and −0.55 μ_B at 9 T). The spin density at the Cr3 and Cr6 sites then changes sign again, and has a similar magnitude to the density at Cr2 and Cr7 (0.33 μ_B at 4.6 T and 0.69 T at 9 T). Almost no spin density is found at the two sites furthest from the Cd site (Cr4 and Cr5) at either measured field. This is very different to NMR spectroscopic results on **3-Cd**, which found a uniform spin density distributed around the Cr sites of that ring (see below).

3.2. EPR Spectroscopy of $\{Cr_7M\}$ Rings

The EPR spectra of both the **3-M** and **4-M** families are very rich.[11,16] The interpretation of these spectra requires us to use a microscopic Hamiltonian approach, where we simulate the spectra using a Hamiltonian based on the local spins and that incorporates both the exchange interaction and the magnetic anisotropy of the individual ions. While we inevitably still discuss the energy levels in terms of the total spin quantum number, *S*, the microscopic Hamiltonian approach implicitly recognizes that such states can be mixed by anisotropic terms in the spin Hamiltonian. Our EPR studies show that the ground states are normally quite pure states, for example, **3-Ni** has a ground state that is 99 % $S = {}^1/_2$ as compared to an isotropic model where *S* is an exact quantum number.[11] The degree of mixing increases for the higher energy excited spin states.

The microscopic Hamiltonian approach reveals the physics much more than the traditional approach (termed either the "strong exchange limit" (SEL) or the "giant spin approximation"). This traditional approach assumes that the exchange interaction is utterly dominant, and that individual total spin states can be treated independently. The magnetic anisotropy of these total spin states is then included as a parameter to simulate the EPR spectra. We have discussed elsewhere the limitations of the SEL approach to compounds **3-M** and **4-M**.[36] The microscopic Hamiltonian approach also has its problems. The main problems concern the size of the Hamiltonian matrices, which can be overcome by various mathematical tricks, and symmetry.[11] As regards the symmetry, in the **3-M** family where there is a *pseudo* fourfold axis

passing through the center of the ring, it is reasonable to set the principle anisotropy axis of individual ions as parallel to this fourfold axis, and to assume that the anisotropy axes of these ions have a similar orientation with respect to this axis. In the chiral **4-M** family there is C_1 symmetry, and we have to make the assumption that all ions have a common orientation of their anisotropy axes;[16] the alternative is to over-parameterize the problem by a vast amount, introducing angles between anisotropy axes.

The results for **3-M** and **4-M** families are given in Table 2, and simulations and measured spectra shown in Figure 17. For

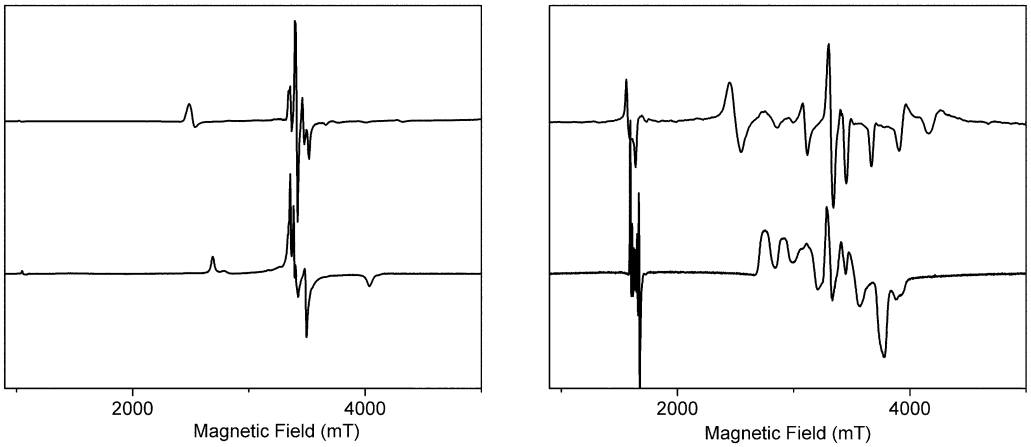

Figure 17. EPR spectra at W-band (17.94 GHz) and 4 K of {Cr_7Zn} (left) and {Cr_7Mn} (right), for the **3-M** (top) and **4-M** (bottom) families.

3-Zn or **4-Zn** at low temperatures we see spectra arising from at least the bottom three states, which in the SEL we would describe as the $S = 3/2$, 1/2, and 5/2 states. For **3-Mn** and **4-Mn** we see spectra arising from the $S = 1$ and $S = 2$ states, and similar spectra are seen for **3-Cu**. For **3-Ni** and **4-Ni** we see only the ground $S = 1/2$ state with weak features from the $S = 3/2$ first excited state which grow in with increasing temperature.

Several proposals have been made that molecular magnets could be used as qubits for quantum information processing.[37–40] One major criticism of such proposals was that they did not take into account the likely coherence times of molecular magnets; there was an assertion that these coherence times would be very short, and therefore it would be impossible to manipulate information stored in the electron spins of molecular magnets before this information was lost to decoherence. Therefore for **3-Ni** and **3-Mn** the coherence time was measured using pulsed EPR spectroscopy at X-band in dilute toluene solutions.[41] The coherence time is essentially the T_2 relaxation time, which can be measured using a standard Hahn echo pulse sequence, $\pi/2$-τ-π-τ-echo. The results show that the T_2 times are much longer than predicted, and that they can be controlled through chemistry.

The most extended study has been performed for derivatives of the $S = 1/2$ ground state **3-Ni**.[41,42] Firstly, the compounds with pivalate and deuterated pivalate were studied, with a common cation—$[Et_2NH_2]^+$. This showed that T_2 varied by a factor of six between the protonated and deuterated form of the complexes. This indicates that the predominant relaxation mechanism is by the hyperfine interaction between the electron spin and the proton spins of the ligands and cation.

Studying the deuterated version of **9-Ni**, that is, with a cesium cation, gives a still higher T_2 value of 15 μs at 1.5 K.[42] This value is far higher than initially predicted, and suggests that further chemical modifications could lead to still higher values. Replacing pivalate with adamantine-carboxylate also leads to a significant increase in T_2, albeit not as dramatic as moving to deuterated pivalate, even though there are now many more ^{1}H nuclei—this is due to the absence of Me groups, the rotation of which provides a relaxation mechanism. However, replacing Me groups with halides does not have such a dramatic effect.[42b] Other groups have since studied several other transition-metal complexes in this context;[43,44] some recent studies have exceeded these values for T_2.[45–47]

All these studies were performed in dilute solution, but it is also possible to show that the heterometallic rings have significant phase-memory times in the solid state.[48] Pulsed EPR studies of **3-Zn** doped into single crystals of diamagnetic $[H_2NMe_2][Ga_7ZnF_8(O_2CtBu)_{16}]$ allow the study of T_2 in the solid state, and also T_2 for several resonances in the $S = 3/2$ ground state EPR spectrum separately. The compounds were not deuterated for this study, so the relaxation times measured are not maximized. The study shows T_2 values of 0.58 to 0.87 μs can be achieved for a doping level of approximately 0.3 %. Increasing the dilution, or perdeuterating samples, or changing the carboxylate or cation, would all increase the T_2 values.

To understand further the source of the decoherence in **3-Ni**, pulsed electron-nuclear double resonance (ENDOR) experiments were performed.[49] The experiments were performed at W-band (95 GHz). The T_2 value was found to be 357 ± 10 ns at this frequency, very similar to the value found at X-band. The observed ^{1}H ENDOR structure can be simulated using a model based on magnetic dipolar contribution to the hyperfine coupling, with the shortest distance of H atoms from the nearest metal ion included in the simulation. This shows that the coupling of electron spins to the H nuclei in the structure is the most significant contribution to decoherence, at least in dilute solutions.

3.3. Solid-State NMR Spectroscopy of {Cr_7M} Rings

The **3-M** family of rings contain several nuclei that are commonly used in NMR spectroscopy, namely ^{1}H and ^{19}F. It is also possible, for some of the compounds, to obtain ^{53}Cr NMR spectra in the solid state.[50] These measurements allow a different approach to understanding the physics of the compounds.

The best place to start is with a study of the ^{53}Cr NMR spectra of **3-Cd** at 1.5 K on a single crystal.[50] The symmetry of **3-Cd** means that there are four unique Cr sites; taking the Cd site as 1, then site 5 is unique, with sites 2 = 8, 3 = 7, and 4 = 6. As the Cd is in the odd sub-lattice, then the spin density at even sites is aligned in the same direction as the spin in the ground state of the molecule ($S_{GS} = 3/2$). The spin density at the three Cr sites in the odd sub-lattice is aligned in the opposite direction to the spin of the ground state.

Three resonance frequencies are seen in the ^{53}Cr NMR spectra of **3-Cd** when measured in fields between 6 and 8 T (high fields are necessary to freeze the electronic spin configuration). One of these resonances has half the intensity of the others and therefore can be identified as being due to Cr4—the site *trans* to cadmium (see Figure 18). The resonance frequency of this site increases with field, and one other resonance shows the same field dependence. This site is therefore due to Cr2 and Cr6, that is, the other two Cr nuclei in the same sub-lattice. The third resonance is much broader and has the opposite field dependence, changing at the same rate but with the resonance frequency decreasing with increasing field. This resonance contains all the Cr nuclei for the even sub-lattice.

As the dependence of the resonance frequency on field is dependent on the local magnetic field (including hyperfine field), the NMR spectra can then be used to calculate the local electron spin density at each Cr site. For the odd sites it is found to be $\langle s_i \rangle = -0.77$, while for the even sites it is found to be $+0.96$. These match well with values evaluated on the basis of the microscopic Hamiltonian for the same compounds. The local magnetic moments ($g\langle s_i \rangle$) of close to 2 μ_B per site differ significantly from the classical picture for a Cr_7Cd ring, where each Cr^{III} site would have $s = 3/2$ hence 3 μ_B per site. The distribution of spin density in **3-Cd** is very different to the spin density in the **6-Cd** as studied by PND (see above),[17d] where almost all the spin density was found on the two Cr sites neighboring the cadmium.

Similar ^{53}Cr-NMR studies on **3-Ni** have been less successful.[51] Only two resonances are seen, which show the same dependence of resonance frequency on magnetic field, which indicates they are in the same sub-lattice as the Ni^{II} ion. The resonances for the Cr nuclei in the even sub-lattice are not observed (they are expected at very low frequencies). The field dependence of the observed frequencies suggest now only 1 μ_B per Cr^{III} site. The NMR results on both **3-Cd** and **3-Ni** show that the magnetic moment arising from the total spin ground state in the heterometallic rings is delocalized over the metal sites in a predictable fashion.

Solid-state ^{19}F NMR spectroscopy performed on single crystals of **2**, **3-Ni**, and **3-Cd** has also been reported.[52] For **2**, at low magnetic fields, a single narrow resonance is seen at the Larmor frequency for ^{19}F, as expected because, owing to symmetry, the $\langle s_i \rangle = 0$ in the $S = 0$ ground state and there is no hyperfine interaction. As the magnetic field is increased parallel to the plane of the ring, four resonances are observed as $\langle s_i \rangle$ becomes non-zero through increasing population of the $M = -1$ component of the $S = 1$ first excited state. The four signals correspond to the magnetically non-equivalent sites (with anisoptropic hyperfine couplings) with the applied field in the plane of the ring. The spectra for **3-Ni** and **3-Cd** are much more complicated because of the lower symmetry and the non-zero and uneven ground state $\langle s_i \rangle$. For example, ^{19}F nuclei bridging Cr···Cd or Cr···Cr edges experience hyperfine fields from one or two nearest neighbors, respectively. All the data can be modeled from the known $\langle s_i \rangle$ distributions to determine the anisotropic hyperfine interactions arising from electron spin density at Cr and, for **3-Ni**, at Ni. These factors make the different F sites highly inequivalent and one result is that—despite the fact that the ^{19}F nuclei are much closer to the electron spin density than ^{1}H—they are much less important in driving electron spin decoherence in Cr_7M because this requires (near) equivalence between sites in nuclear spin "flip-flop" transitions.

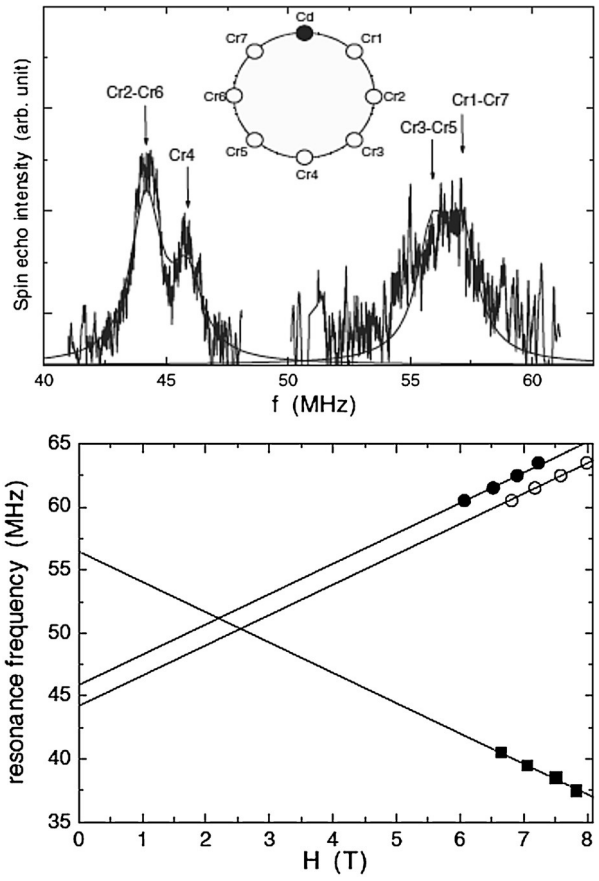

Figure 18. Solid-state ^{53}Cr-NMR of **3-Cd**. Top: ^{53}Cr-NMR spectrum normalized to zero-field at $T = 1.5$ K. The inset gives the numbering scheme for the Cr sites. Bottom: ^{53}Cr resonance frequency in a single crystal of **3-Cd** at $T = 1.5$ K as a function of an applied magnetic field perpendicular to the plane of the molecule. Taken from Ref. [50] with permission.

3.4. Physical Studies of $\{Cr_xCu_2\}$ Rings

The larger $\{Cr_{10}Cu_2\}$ (**19**) and $\{Cr_{12}Cu_2\}$ (**20**) rings offer a somewhat different challenge to the $\{Cr_7M\}$ rings. The presence of two heterometals in the structure at ordered positions leads to a more complicated sub-lattice structure. There is also the question of whether, as in **3-Cu**, we have a mixture of ferro- and anti-ferromagnetic exchange between the Cr and Cu spin centers. The combination of these factors leads to the curious observation that in $\{Cr_{10}Cu_2\}$ the spin ground state is lower where ferromagnetic exchange is present than where exchange is exclusively anti-ferromagnetic.[23]

As the copper sites in **19** are separated by $\{Cr_5\}$ chains, then the copper atoms would be at sites 1 and 7 in the ring, that is, both in the same sub-lattice (Figure 19). Therefore for exclusively anti-ferromagnetic (AF) exchange, the odd sub-lattice has a spin given by $4\times3/2+2\times1/2=7$ (Figure 19a). The even sub-lattice contains exclusively Cr^{III} centers, so the spin would be $6\times3/2=9$. Therefore the spin ground state would be $S=2$. If, however, there is ferromagnetic exchange present between copper and one-neighboring Cr site, this changes the magnetic structure, and the spin ground state would be $S=0$ (Figure 19b). For **20**, the copper sites are separated by $\{Cr_6\}$ chains, which means the reverse is true as one copper is in the odd sub-lattice and the other in the even sub-lattice. Thus with all anti-ferromagnetic exchange, $S_{GS}=0$ for **20**, and the presence of ferromagnetic exchange will give $S_{GS}=1$.

Physical studies show this simple picture to be correct.[24] Modeling magnetic measurements required use of quantum Monte Carlo (QMC) methods owing to the size of the molecules, however the speed of QMC methods also allowed a more detailed examination of the parameters used than can be achieved with more conventional magnetic fitting tools. The best fit of the data is achieved with: $J_{CrCr}=-5.14\pm0.35$, $J_{Cr\text{-}Cu(1)}=-18.4\pm4.2$, $J_{Cr\text{-}Cu(2)}=+4.1\pm1.4\ cm^{-1}$ for **19** and $J_{CrCr}=-5.21\pm0.35$, $J_{Cr\text{-}Cu(1)}=-22.6\pm5.6$, $J_{Cr\text{-}Cu(2)}=+1.74\pm3.5\ cm^{-1}$ for **20**. It is noticeable that as in **3-Cu** one ferro- and one anti-ferromagnetic exchange is found between Cr and Cu. For **20** these spin Hamiltonian parameters are confirmed by INS spectroscopy.[53]

The knowledge of the spin Hamiltonian parameters in these cyclic but non-simple systems has allowed the use of a novel technique to study molecular magnets, low-temperature tunnel-diode resonator (TDR) measurements,[53,54] and measures directly the in-phase susceptibility, χ'. These measurements involve radio-frequency (15 MHz) irradiation of the sample at $T=55$ mK, and measure the frequency shift of this frequency as a function of applied field, which depends on χ'. TDR measurements on **19** show peaks at specific values of magnetic field; some of peaks are equivalent to the steps seen for **1** and **2** in torque magnetometry.[1,6] However, whereas torque magnetometry only shows peaks for ground-state crossings, that is, for critical fields where the ground-state spin of the molecule changes, the TDR measurements shows peaks at level crossings between excited states (Figure 20).[53,54] Such excited-state crossings should not effect the equilibrium variation of magnetization with field, but are clearly observed by TDR. Presumably this is because TDR is measuring the dynamic susceptibility of compounds, hence revealing features not observed in static measurements. The technique has not, to our knowledge, been used further for magnetic molecules.

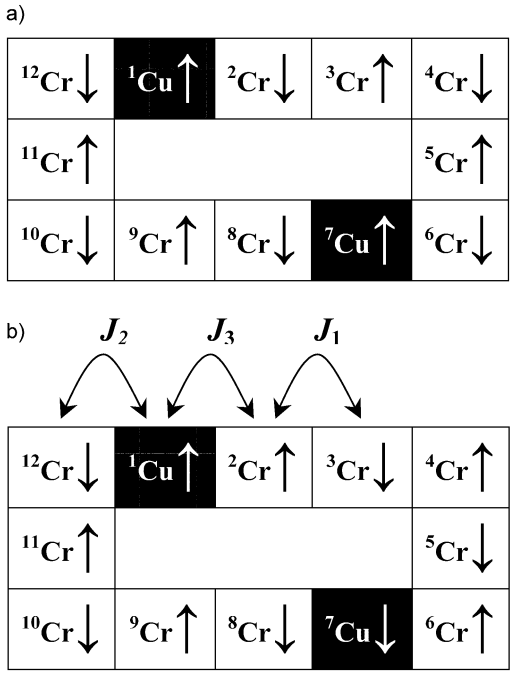

Figure 19. The possible spin structures for the ground state of **19**. a) All AF-exchange, leading to an $S=2$ ground state. b) Two ferromagnetic Cr-Cu exchange interactions, leading to an $S=0$ ground state.

3.5. Deposition of $\{Cr_7Ni\}$ Rings on Surfaces

Studies of molecular magnets deposited on surfaces is a major topic for research[55–58] as it is felt that most likely applications will require the ability to address individual molecules, probably by some form of scanning tunneling microscopy. The **3-Ni** heterometallic rings are ideal for such studies as a result of their combination of high stability, high solubility, and surprisingly high vapor pressure which allows them to be sublimed. The presence of two different metals also allows element-sensitive measurements, such as X-ray magnetic circular dichroism (XMCD). The rings can therefore be deposited either from the solution phase or the gas phase, and their magnetic properties studied by XMCD.

The ability to functionalize the **3-Ni** structure allows inclusion of groups that can potentially bind to specific surfaces. Four versions of the ring have been studied, deposited from THF solution onto gold:[59] these include the ring containing 3-thiophene carboxylate (3-tpc) in place of pivalate $[NH_2{}^nPr_2][Cr_7NiF_8(3\text{-tpc})_{16}]$ (**3-Ni-tpc**). X-ray absorption spectroscopy (XAS) and XMCD were performed on both multi-layer films and sub-monolayers. The studies show the same Cr:Ni ratio as in the precursor, suggesting molecules are deposited intact. However, there is evidence for additional sulfur-containing molecules being present, which is

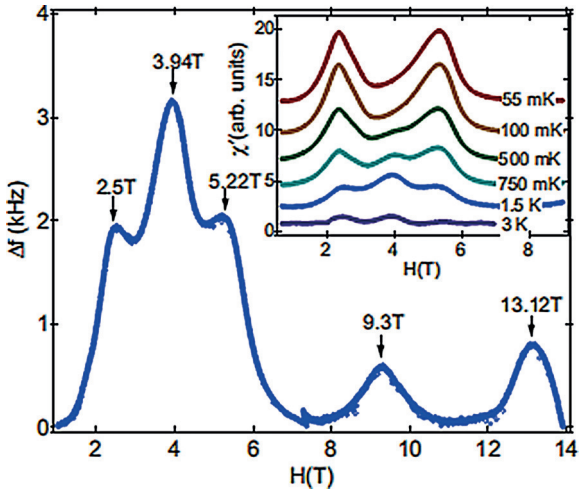

Figure 20. TDR measurements on **19** after background subtraction at $T = 1.5$ K. The field values for observed peaks are indicated. The peaks at approximately 2.5, 5.22, and 13.12 T are ground-state crossings; the peaks at 3.94 and 9.3 T are excited-state crossings. Inset: TDR signal after background subtraction at the temperatures marked. Taken from Ref. [53] with permission.

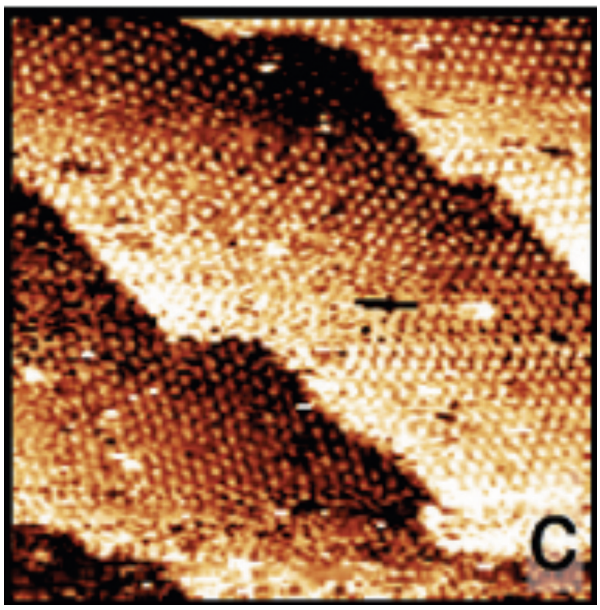

Figure 21. Scanning tunneling microscope images of a complete self-assembled monolayer of **3-Ni** on a clean Au^{III} surface

probably thiophene from decomposition of some ligands. In the most studied sample, **3-Ni-tpc**, the magnetic exchange interactions were found to be smaller, in particular the magnetic exchange between Cr^{III} and Ni^{II} is reduced to one-third of the value found in the bulk sample. Further studies are needed to determine whether this reduction is due to distortion of the compound, or due to some form of interaction with the surface.

While thiols enable deposition on gold, addition of long alkyl-chains to the carboxylate ligands allow successful deposition on highly ordered pyrolytic graphite (HOPG).[60] Several examples were made of $[NH_2{}^nPr_2][Cr_7NiF_8(O_2CR)_{16}]$ compounds, including R = -CH(Et)(C_5H_{11}), -CH(C_9H_{19})-(C_7H_{15}), *o*-C_6H_4-O-Ph. When deposited from 10^{-4} M solutions in toluene, sub mono-layers are again formed. 3D aggregates show a higher tendency to form when the rings contain *ortho*-phenoxybenzoate, presumably owing to interaction between the aromatic ligands. XPS experiments demonstrate that the rings are intact on deposition. A firmer attachment to the surface can be achieved by functionalizing the surface with an anionic self-assembled monolayer. The ring is then functionalized with a single zwitterionic carboxylate, betaine, which leads to the ring being neutral, and once the central dipropylammonium cation is considered the whole assembly is a cation. This binds well to the anionic surface layer.[60]

The parent ring, **3-Ni**, can be sublimed intact onto gold surfaces.[61] On Au(111) ordered monolayers are formed, which have a herringbone modulation reflecting the structure of the gold surface beneath (Figure 21). Again XPS shows that the molecules are sublimed intact. Unlike in liquid-phase deposition there is no evidence for additional sulfur-containing molecules, therefore this technique seems preferable for deposition of these large polymetallic compounds.

4. Heterometallic Rings as Lewis Acids

The **4-M** family of heterometallic rings contain a single monodentate ligand attached to the M^{II} site. As made this ligand is water, and this is easily displaced. Typically 4-phenylpyridine has been used to produce rings that are stable and on which detailed physical studies can be performed. However as it is possible to displace these ligands with pyridine, it is equally straightforward to displace the monodentate ligand with di-imines, and hence link together two rings producing a supramolecule with a tunable intra-qubit interaction.[15,62–65]

This has been done with a range of di-imines[62,63] to study the interaction between **4-Ni** rings (Figure 22). The di-imines include pyrazine, 4,4′-bipyridyl, (PyPy), 3,3′,5,5′-tetramethyl-4,4′-bipyridine,[63] *trans*-1,2-dipyridylethene ($PyMe_2PyMe_2$), 3,8-phenanthroline (phen),[63] 1,2-dipyridylethene (Py-CH = CH-Py), 1,2-dipyridylethane, (Py-CH_2-CH_2-Py), dipyridylacetylene, (Py-C ≡ C-Py), *meso*-alpha,- beta-bispyridylglycol, (Py-CH(OH)-CH(OH)-Py), 4,4′- azopyridine, (Py-N = N-Py), 1,4-dipyridylbenzene, (Py-Bz-Py), 3,6-dipyridyl-s-tetrazene, (Py-Tz-Py), bis-1,4-(4-pyridylvinyl)benzene, (Py-CH = CH-Bz-CH = CH-Py). 4,4′-bi-3,5-dimethylpyrazole (PzPz) and 4-(1*H*-pyrazol-4-yl)pyridine (PzPy),[63] which involve five-membered heterocycles were also investigated. These results show that the ring···ring interaction can be controlled by distance,[62] by the planarity of the di-imine bridge,[63] and by the type of heterocycle present. As the exchange interaction is too small to be studied by conventional magnetic measurements two studies were pursued: continuous wave (cw) EPR spectroscopy and very low-temperature magnetic measurements.[64]

Distance is the most straightforward property to study.[62] Pyrazine provides the shortest link, giving a Ni···Ni contact in [(**4-Ni**)$_2$-pyrazine] of 7.0 Å. If we restrict ourselves to six-

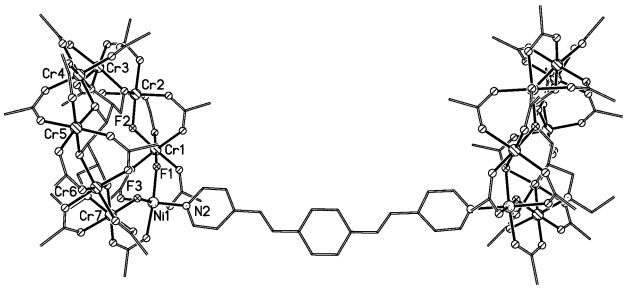

Figure 22. The structure of a dimer of **4-Ni** rings linked by bis-1,4-(4-pyridylvinyl)benzene. Shading as Figure 1. H-atoms and Me groups excluded for clarity.

membered heterocycles the next shortest links are in [(**4-Ni**)$_2$-PyPy], [(**4-Ni**)$_2$-PyMe$_2$PyMe$_2$], and [(**4-Ni**)$_2$-phen], where the Ni···Ni contact is around 11.2 Å. For [(**4-Ni**)$_2$-Py-CHCH-Py] the distance is longer at 11.4 Å, and for all other compounds longer still, for example, in [(**4-Ni**)$_2$-Py-Tz-Py] the Ni···Ni distance is 15.2 Å.

For the [(**4-Ni**)$_2$-pyrazine] the magnetic exchange interaction can be measured directly by magnetization measurements at 40 mK, and is around $-0.7\ cm^{-1}$. For [(**4-Ni**)$_2$-PyPy] the measured value falls to $-0.11\ cm^{-1}$ and for [(**4-Ni**)$_2$-Py-CHCH-Py] it falls a little further to $-0.10\ cm^{-1}$. For [(**4-Ni**)$_2$-Py-Tz-Py] no interaction can be measured by low-temperature magnetization. These direct measurements are supported by cw-EPR measurements; as the exchange is weak and anti-ferromagnetic, the supramolecular dimers of heterometallic rings have $S=0$ ground states but nearby $S=1$ excited states. The zero-field splitting of the $S=1$ ($D_{S=1}$) states can be related directly to the size of the magnetic exchange.

EPR measurements allow us to examine the role of the torsion angle in the di-imine link. When **4-Ni** is linked by phen the link is essentially flat. With PyPy the twist angle between the two pyridine rings is around 41° while with PyMe$_2$PyMe$_2$ this angle is 82°. The EPR studies show that $D_{S=1}$ varies from $+0.017\ cm^{-1}$ for [(**4-Ni**)$_2$-phen] to $+0.013\ cm^{-1}$ for [(**4-Ni**)$_2$-PyPy] to $<0.001\ cm^{-1}$ for [(**4-Ni**)$_2$-PyMe$_2$PyMe$_2$].[63] This sequence suggests that the exchange interaction we are measuring by low-temperature magnetization and by cw-EPR spectroscopy has a significant super-exchange component, that is, the exchange is mediated by the delocalized π-electrons of the di-imine link. DFT calculations in which the twist angle was varied systematically suggests that the magnetic coupling between the rings follows a cos^2 dependence on the twist angle, in a manner analogous to that reported for charge transport through aromatic groups.[65]

Further evidence for the importance of super-exchange through the organic linker comes from studies of compounds where the links contain five-membered rings: [(**4-Ni**)$_2$-PzPz] and [(**4-Ni**)$_2$-PzPy].[62,63] In both cases $D_{S=1}$ is not observed by cw-EPR spectroscopy, meaning the parameter is less than $0.001\ cm^{-1}$. A simple picture based on the spin alternation rule around five-membered heterocycles can explain why no super-exchange is observed in these later two dimers.

These studies show we can tune the ring–ring interaction quite precisely, which is extremely important in pursuing the idea that such rings can be used as qubits. Recent work has focused on the coherence times of rings,[41–47] but the timescale associated with the ring–ring interaction is also vital.[66] The time needed to perform a two-qubit gate (the gate time) is indirectly proportional to the strength of the magnetic interaction. For any successful quantum computer we need to control this value precisely; it has to be much shorter than the coherence time, as manipulations must be performed before the information is lost through decohence. However, it must be longer than the time needed to manipulate a single spin; we are using pulsed EPR spectroscopy to manipulate the spins, so this time is around 10 ns using commercially available pulsed EPR spectrometers.

If we consider [(**4-Ni**)$_2$-PyPy)] as an example, the coupling is $-0.11\ cm^{-1}$ and this converts into a gate time of 0.25 ns;[62] the coupling is strong enough that we cannot manipulate individual qubits separately from manipulating the dimer. Therefore other links have been designed to separate the **4-Ni** rings further. To measure such interactions requires a pulsed EPR technique called double electron–electron resonance (DEER), which is widely used in structural biology to study distances between radicals. In our systems the distance is known, it is the magnitude of the interaction that is of importance.

To vary the interaction systematically we turned to boronic acid capped clathrochelate complexes synthesized by Severin and co-workers.[67] These compounds contain one or two low-spin Fe^{II} ions within the bridge, and we can systematically vary the Ni···Ni distance from 18.9 Å in the shortest case, to 27.1 and then 30.7 Å (Figure 23).[66] For all

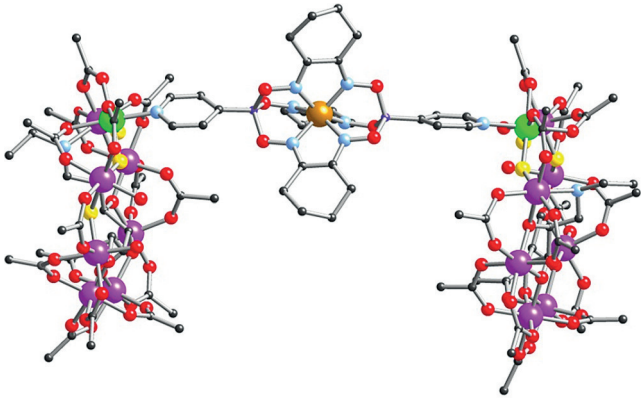

Figure 23. The structure of two **4-Ni** rings linked by a clathrochelate group containing low-spin Fe^{II}. The Ni···Ni distance is 1.9 nm. Cr purple; Ni green; F yellow; N blue; O red; B dark purple; C black. H-atoms and Me-groups omitted for clarity.

three of these compounds the cw-EPR spectroscopy shows no evidence of coupling. However, by pulsed EPR spectroscopy we can measure a coherence time for each **4-Ni** unit, and then use DEER spectroscopy to measure the two-qubit gate time. The coherence time, which is not optimized, is around 600 ns in each case. For the longest link, the two-qubit gate time is 550 ns. This time is too long, as it approaches the coherence time. For the shortest link the two-qubit gate time is 157 ns,

significantly shorter than the coherence time. Thus through supramolecular chemistry we can vary the gate time from far too short in [(**4-Ni**)$_2$-PyPy] to too long, with the longest clathrochelate link, to just right. Other approaches to quantum computing do not have this ability to control both coherence times and gate times.

While the ability to produce dimers of rings has been taken forward to control the inter-qubit interaction, other aspects of this chemistry remain unexploited. The **4-M** rings bind well to any pyridine-based ligand. Thus other poly-pyridyl ligands could be used to make larger assemblies. The only example where this has been reported involves using 5,10,15,20-tetra(4-pyridyl)porphyrin as the bridge, and four **4-Ni** rings are easily assembled about this unit (Figure 24).[15] No physical studies have yet been reported on this larger four-qubit ensemble.

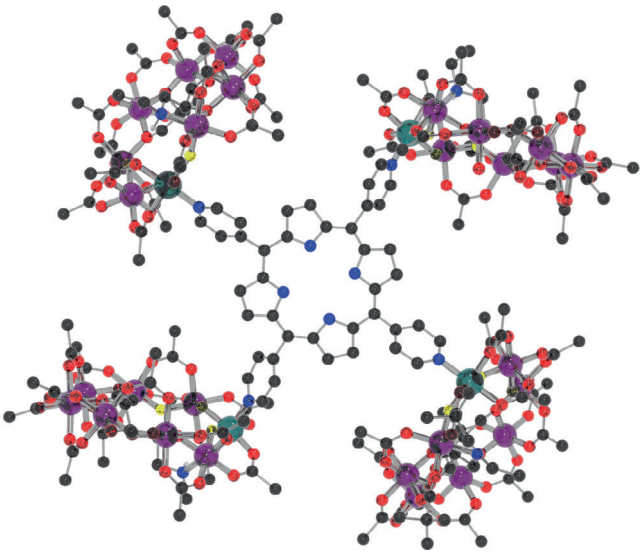

Figure 24. The structure of four **4-Ni** rings assembled about 5,10,15,20-tetra(4-pyridyl)porphyrin. Colors as Figure 23. H-atoms and Me-groups omitted for clarity.

5. Heterometallic Rings as Components of Hybrid Rotaxanes

The presence of the templating ammonium cations in these structures resembles some of the structural features of rotaxanes, and it was comparatively straightforward to make pseudo-[3]rotaxanes using simple diamines, for example, 1,8-diaminooctane.[68] Slightly more sophisticated pseudo-[3]rotaxanes can be made by using [EtNH$_2$CH$_2$-py]$^+$ as the template; the pyridine group of the template can act as a ligand, for example, binding to [M$_2$(O$_2$C^{t}Bu)$_4$] compounds (M = Ni, Co, Cu).[68]

The first hybrid organic–inorganic rotaxane involved more sophisticated organic threads,[69] synthesized by Leigh and co-workers. Two threads were studied, one containing a single amine site, to be protonated to act as a template, and the other containing two amines. After reaction with hydrated chromium trifluoride and a dicobalt(II) complex, a [2]rotaxane of the first thread, and [2]- and [3]rotaxanes of the second thread could be made. By making the Cr$_7$Co rings it was possible to study the motion of the compounds in solution by NMR spectroscopy. In the [2]rotaxane with two ammonium positions it was found that the Cr$_7$Co ring shuttles between the two positions at a rate of around 1.2 s^{-1}, while the spinning of the ring about each thread is extremely fast.[69]

The flexibility of this chemistry allows a [4]rotaxane to be made using the di-amine thread; this involves using copper carbonate as the source of the divalent metal, resulting in two Cr$_{10}$Cu$_2$ rings forming about two organic threads (Figure 25).

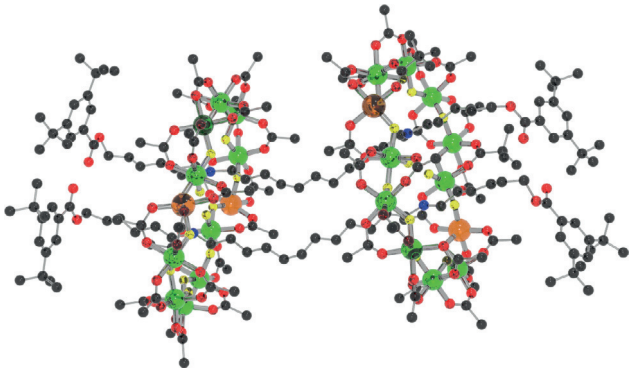

Figure 25. The structure of a [4]rotaxane involving two {Cr$_{10}$Cu$_2$} rings, linked by organic threads. Colors as Figure 8, with Cu orange. H-atoms excluded for clarity.

These rings are very similar to those found in **19**. This [4]rotaxane can be made in 37% yield, which is an unusually high yield for such an interlocked structure.[69] Further studies have reported ways to increase the yields of the [2]rotaxanes, and to understand the mechanism by which these hybrid structures form.[70]

The ability to make [3]rotaxanes also allows us to study the interaction between **3-Ni** rings where there is no direct covalent bond present.[66] This arrangement excludes any possibility of super-exchange being a path for a magnetic interaction, which is clearly important in dimers of **4-Ni** rings discussed above. The first thread designed has three phenyl groups between the ammonium centers to ensure rigidity, [RCH$_2$CH$_2$NHCH$_2$(C$_6$H$_4$)$_3$CH$_2$NHCH$_2$CH$_2$R] (R = Ph or ^{i}Pr). The [3]rotaxanes grown about this thread have ring···ring separations of 16.4 Å. The ease with which the [3]rotaxanes can be made allows us to incorporate carboxylates in the **3-Ni** rings that increase coherence times. Using either deuterated pivalic acid or 1-adamantane carboxylate as the ligand in [Cr$_7$NiF$_8$(O$_2$CR)$_{16}$]$^-$ rings allow us to make supramolecules where the coherence times for the spins are 2400–3300 ns, and the gate time is of around 80 ns.[66] Such a system is an excellent candidate for performing simple algorithms as the gate time is longer than the time to manipulate a single spin, while the coherence times are forty-times longer. Chemistry allows us to control the coherence times and independently control the gate times, parameters which cannot be controlled so easily in other possible implementation schemes.

The threads of the rotaxanes can also be functionalized so that the hybrid rotaxanes can act as ligands. To demonstrate

this principle, threads containing pyridine groups as stoppers have been synthesized. These include [{Py$(CH_2)_n$NH-$(CH_2)_{10}$NH$(CH_2)_n$Py}] ($n=1$ or 2).[71] When treated with mono- or di-metallic copper complexes, for example, Cu-$(hfac)_2$ or $[Cu_2(O_2C^tBu)_4]$, 1D coordination polymers can be synthesized, which involve [3]rotaxanes as part of the structure (Figure 26). This is somewhat different to the

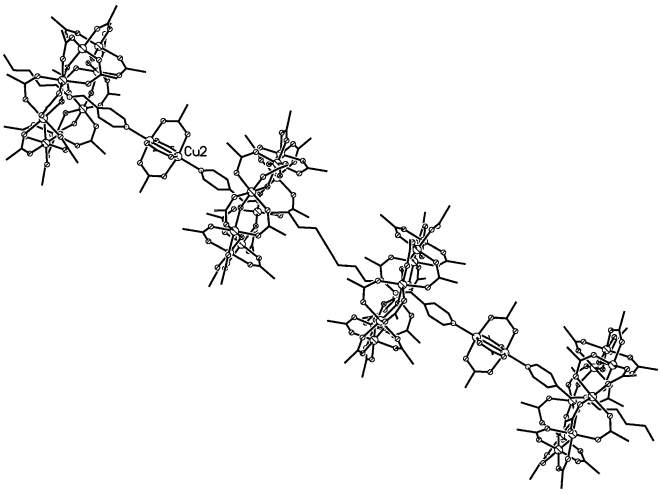

Figure 26. A polymer involving [3]rotaxanes involving **3-Ni**, linked by $[Cu_2(O_2C^tBu)_4]$. Shading as Figure 1. H-atoms and Me groups excluded for clarity.

metal–organic rotaxane frameworks reported by Loeb and co-workers.[72] These compounds begin to approach the structural complexity required for a proposal by Santini et al. to use 1D ensembles of molecular magnets as quantum simulators.[73]

It has also been possible to deposit [*n*]rotaxanes on surfaces.[74] Both [2]- and [3]rotaxanes are found to bind to gold surfaces, and the functionalization of the rotaxanes can control how the complex binds to the surfaces. Characterization by XPS and STM measurements show the compounds are intact, and also suggest that the [2]rotaxanes, where the rings are bound to the surface through a sulfur group attached to the organic thread, form more stable surface layers than the simpler rings that had previously been studied.[59]

Very recently a slightly more complicated interlocked structure has been reported—a hybrid inorganic–organic daisy chain.[75] Purely organic daisy chains were reported by Stoddart and co-workers at the end of the 1990s.[76] The structures are formed when the thread of one rotaxane binds to the ring of a neighboring rotaxane; in our case, a thread involving a terminal pyridine group is used in a reaction intended to make a [2]rotaxane involving a $\{Cr_7Zn\}$ ring. Instead a daisy chain forms, in which the pyridine binds to a Zn^{II} site in a neighboring ring (Figure 27). The result is a compound $[Cr_6Zn_2(\mu\text{-}F)_8(O_2C^tBu)_{15}(Py\text{-}C_6H_4\text{-}CH_2\text{-}NH_2\text{-}C_2H_4\text{-}Ph]_2$ (**35**); one of the two Zn sites is five-coordinate, and bound to the pyridyl-donor from the thread. The other Zn site is disordered around the ring giving at least two isomers, in an analogous manner to that found for **12-Ni**.[20]

[2]rotaxanes and [3]rotaxanes with threads terminated by a pyridine can also act as ligands for mononuclear copper sites, giving discrete molecules rather than 1D-polymers.[77] If $[Cu(hfac)_2]$ is used a single [2]rotaxane can bind to give $\{[Cu(hfac)_2][PyCH_2NH_2CH_2CH_2Ph][Cr_7NiF_8(O_2C^tBu)_{16}]\}$ (**36**) while $Cu(NO_3)_2{\cdot}3H_2O$ reacts to give $[Cu(NO_3)_2(Me_2CO)]\{[PyCH_2NH_2CH_2CH_2Et][Cr_7NiF_8(O_2C^tBu)_{16}]\}_2$ (**37**). The EPR spectroscopy of these compounds is very clear,

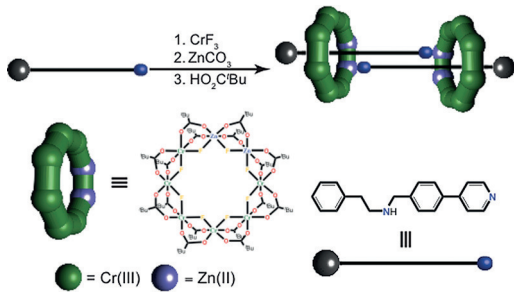

Figure 27. A schematic description of the formation of a hybrid inorganic–organic daisy chain **35**. Modified from Ref. [75] with permission.

because the difference in the *g*-values between the two spin 1/2 centers (Cu^{II} and Cr_7Ni) leads to the Zeeman energies being greater than the spin–spin interaction. Thus when one [2]rotaxane is bound to a copper an AB spin system results, whereas when two [2]rotaxanes are bound to a copper an AB_2 spin system results (Figure 28). The result are spectra where the fine structure is resolved in a manner analogous to NMR spectroscopy.[77]

6. Heterometallic Rings as Ligands

The next step in developing the chemistry of the heterometallic rings is to include functional groups within the carboxylate ligands that allows them to act as ligands for other metal complexes.[78–82] This works remarkably well because of the different reactivity of complexes of trivalent chromium and complexes of divalent metals. If the rate of aquation is considered as an example, Cr^{3+} exchanges water ligands around 10^{10} times more slowly than Ni^{2+}.[83] This means that any substitution reactions involving the carboxylates on the exterior of the heterometallic rings will take place on the Cr···M edges, and not on the Cr···Cr edges. As there are four carboxylates on these edges, it is possible to replace up to four carboxylates and, in some instances, to separate the resulting products.

The first such chemistry pursued involved inclusion of *iso*-nicotinate (O_2C-Py) as the functionalized carboxylate.[78–80] Reaction of *iso*-nicotinic acid with $[R_2NH_2][Cr_7NiF_8(O_2C^tBu)_{16}]$ in a slightly polar solvent produces compounds of formula $[R_2NH_2][Cr_7NiF_8(O_2C^tBu)_{16-x}(O_2C\text{-}Py)_x]$ (where $x=0, 1, 2, 3, 4$). The differently substituted compounds can be separated, and in the case of the disubstituted case even isomers can be separated by chromatography.

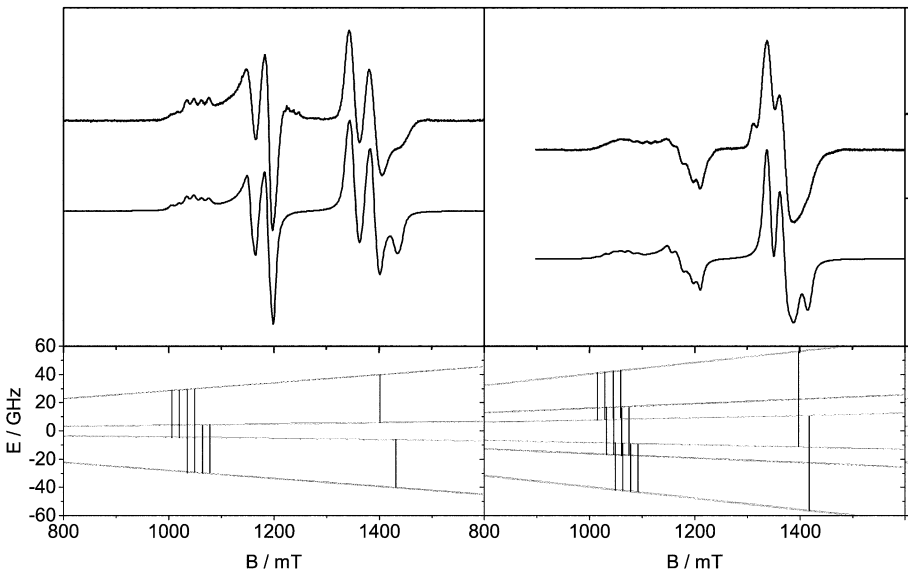

Figure 28. Q-band EPR spectra of **36** (left) and **37** (right); experimental spectra top, simulations below and energy levels shown at the bottom. Modified from Ref. [77] with permission.

The best yield is found for $x = 1$, that is, the mono-substituted compound (**3-Ni-Py**) in which the *iso*-nicotinate is found perpendicular to the plane of the $\{Cr_7Ni\}$ ring.

Two **3-Ni-Py** molecules can bind to monometallic Cu^{2+} complex, making a supramolecule with a *trans*-arrangement of the **3-Ni-Py** ligands (Figure 29 a).[75] This compound has three $S = 1/2$ groups weakly interacting. This can be seen in beautifully resolved Q-band EPR spectra; coupling three $S = 1/2$ centers gives two spin doublets and one spin quartet and features arising from each of these spin multiplets are seen (Figure 29 b). Such a spin system can be parameterized in a variety of ways but the most rigorous simulation involves taking all seventeen paramagnetic centers in the system into account and gives an isotropic exchange interaction between the Cu^{2+} and the rings of $+0.15\ cm^{-1}$, with an anisotropic exchange interaction of $+0.01\ cm^{-1}$. If two **3-Ni-Py** molecules are bound to a dinuclear copper complex, in which there is strong anti-ferromagnetic exchange between the copper centers, no evidence of an exchange interaction is seen in the cw-EPR spectra.[78] This suggests a possible switching mechanism, between cases where there is a diamagnetic bridge and a paramagnetic bridge.

This idea has been taken further by performing detailed calculations on supramolecules in which two **3-Ni-Py** molecules are bound to Ni^{2+} complexes.[79] In these cases both *cis*- and *trans*-isomers are found. Other structural features can be subtly modified, for example pyradizine-4-carboxylate can be used in place of *iso*-nicotinate, and where the electronic structure of the Ni center can be varied by used of different β-diketonates. This ability to control precisely the interaction between spin centers is important. Calculations suggest these compounds have the correct characteristics to be used as components of quantum simulators.[73]

The pyridine of **3-Ni-Py** can also act as a ligand for trimetallic, hexametallic, and dodecametallic cage complexes (Figure 30).[80] In each case the $\{Cr_7Ni\}$ ring is unchanged from **3-Ni**. Equally, the polymetallic cages to which the substituted ring binds are unchanged. The arrays

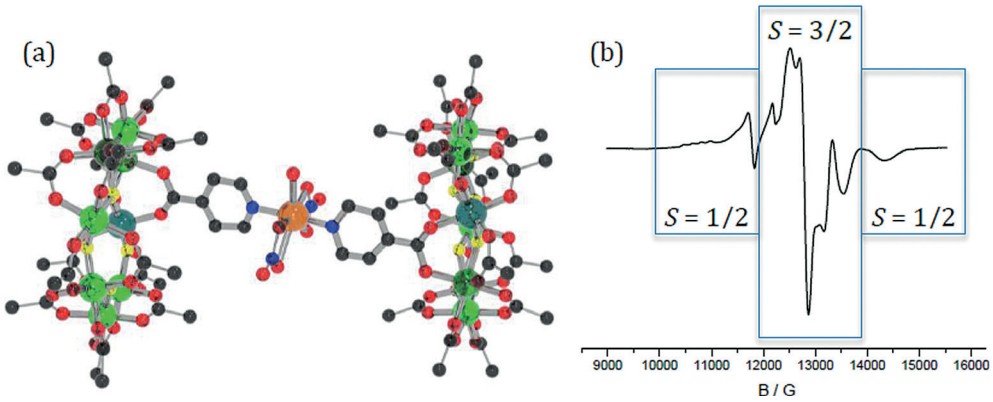

Figure 29. a) The structure of $[\{\textbf{3-Ni-Py}\}_2(Cu(NO_3)_2(acetone)]$. Colors as Figure 25. H-atoms and Me groups excluded for clarity. b) The Q-band EPR spectrum of $[\{\textbf{3-Ni-Py}\}_2(Cu(NO_3)_2(acetone)]$ as a powder, recorded at 4.2 K. The features are associated with the spin states indicated.

that result suggest a route to very large heterometallic cage complexes, for example, the complex of **3-Ni-Py** bound to a $\{Ni_{12}\}$ ring contains sixty metal centers (Figure 30). The degree of control achieved in making such a large heterometallic cage of cages is remarkable. There is a weak magnetic interaction between the $S = 1/2$ **3-Ni** ring in this compound and the $\{Ni_{12}\}$ ring which has an $S = 12$ ground state.

The next mono-substituted complex reported involves introduction of *iso*-phthalic acid in an analogous manner to *iso*-nicotinate.[81] The compound $[^nPr_2NH_2][Cr_7NiF_8(O_2C^tBu)_{15}(O_2CC_6H_4CO_2H)]$ (**3-Ni-CO_2H**), forms in a moderate yield (26 %) and forms a strong hydrogen bond between the two phthalate groups. To use this substituted ring as a ligand it is best to deprotonate the carboxylic acid, using piperidine or tetramethylpiperidine. This produces a salt where the piperdinium cation is involved in the H-bonding. The salts react smoothly with either copper(II) or zinc(II)

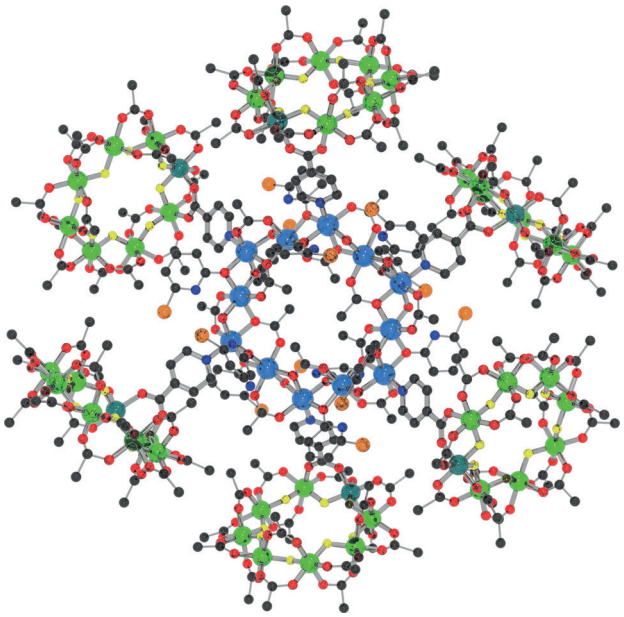

Figure 30. A $\{Ni_{12}\}$ ring surrounded by six **3-Ni-Py** ligands. Colors as Figure 8, plus central Ni ions light blue, Cl orange. H-atoms and Me groups excluded for clarity.

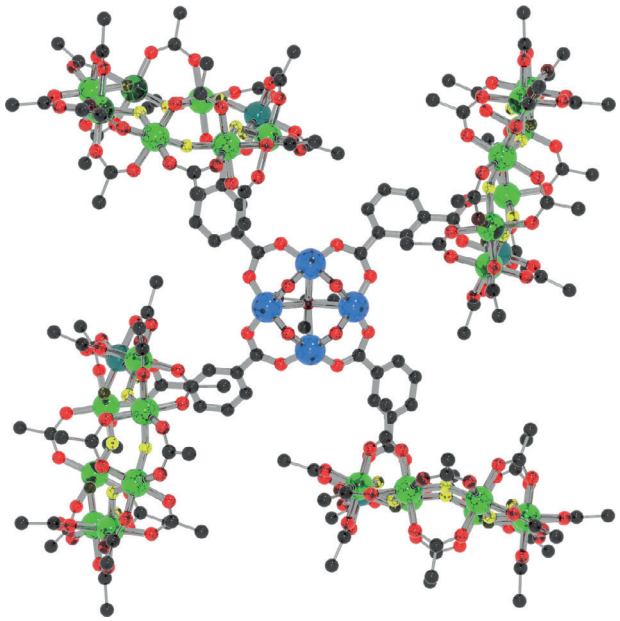

Figure 31. A $\{Cu_4\}$ square coordinated by four **3-Ni-CO$_2^-$** ligands. Colors as Figure 8, plus Cu light blue.

perchlorate to produce compounds in which there is a tetrametallic copper or zinc core bound to the **3-Ni-CO$_2^-$** ligands. In the copper case, the four copper(II) centers form a square, with four **3-Ni-CO$_2^-$** ligands bound on the four edges (Figure 31). In the zinc case, an oxo-centered Zn_4 tetrahedron is stabilized by six **3-Ni-CO$_2^-$** groups, with one on each edge.[81] This is the zinc oxyacetate structure. These mono-substituted rings appears to behave as sterically demanding, and very highly soluble, versions of the simple pyridine or carboxylate ligands.

Two isomers of the di-substituted *iso*-nicotinate ring have also been studied.[71,82] The first has the two *iso*-nicotinates on neighboring edges of the ring, pointing above and below the $\{Cr_7Ni\}$ plane. This compound therefore has some similarities to 4,4′-bipyridyl, and forms simple 1D-polymers either with mononuclear complexes, or dinuclear $[Cu_2(O_2C^tBu)_4]$ units.[71] With an oxo-centered metal triangle, for example, $[Fe_2CoO(O_2C^tBu)_6]$ the di-substituted ring can form a 3D-porous coordination polymer (Figure 32). The structure is a 10,3b-net, as could be predicted for a bulky linear link between triangular nodes.[82] The 10,3b-net is interpenetrating, and has huge solvent voids in the lattice with around 50% of the crystal consisting of disordered solvent.

The second isomer studied has both *iso*-nicotinates on the same edge of the $\{Cr_7Ni\}$ ring.[71] The reaction of this isomer with copper(II) nitrate produces a 1D polymer, but with a complicated structure (Figure 33). The structure alternates between squares, made of two Cu^{2+} sites and two rings, and single copper sites. At the single copper sites the rings are *trans*- with the remaining coordination sites occupied by nitrates. Within the squares, three pyridines from rings bind to each copper site. These initial results suggest there could be very interesting coordination polymers made by reaction of these di-substituted rings with suitable metal nodes.

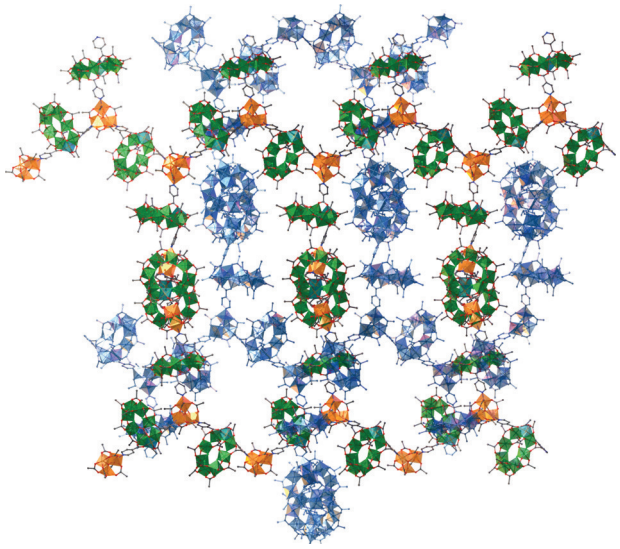

Figure 32. An interpenetrating (10,3b) net formed from reaction of a di-*iso*-nicotinate substituted $\{Cr_7Ni\}$ ring and an oxo-centered triangle, $\{Fe_2CoO(O_2C^tBu)_6\}$. One net is colored blue, in the second net the ring is colored green, and the oxo-centered triangle orange.

A further development arises from performing organic chemistry on functional groups attached to **3-Ni**.[84] The idea was inspired by the Pd capsules reported by the Stang and Fujita groups,[85] and involves creating a ligand that incorporates **3-Ni** and that can then produce a Pd capsule. Firstly, 4′-hydroxy-4-biphenylcarboxylic acid is introduced on one Cr···Ni edge of **3-Ni**, and then a series of organic reactions performed to produce a version terminated in a widely spaced di-pyridyl ligand (Figure 34a). The eventual compound $[^nPr_2NH_2][Cr_7NiF_8(O_2C^tBu)_{15}(O_2C\text{-}C_6H_4\text{-}C_6H_4\text{-}OC(O)\text{-}3,5\text{-}$

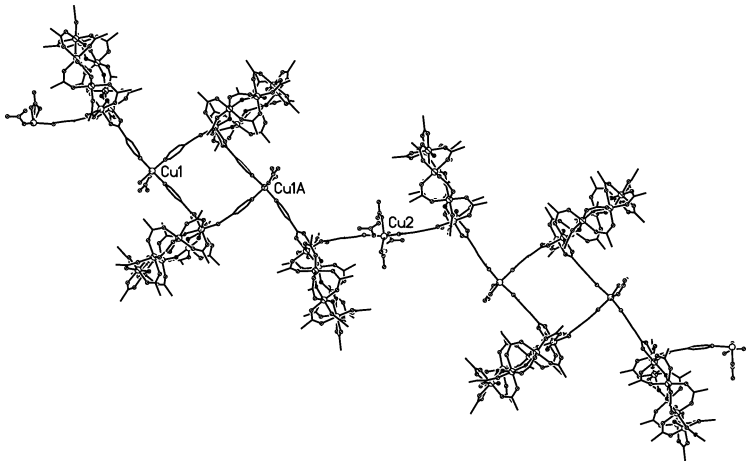

Figure 33. The structure of a 1D-polymer formed from a di-*iso*-nicotinate substituted ring and mononuclear copper nodes.

$C_6H_3(C{\equiv}C\text{-}Py)_2$] (**3-Ni**-$Py_2$) can then react to produce a capsule compound [Pd_{12}(**3-Ni**-Py_2)$_{24}$] (Figure 34b). The compound contains over 200 metal centers, and has a diameter of over 8 nm as measured by a variety of solution techniques including diffusion-ordered NMR spectroscopy and small-angle X-ray scattering; as such it is one of the largest molecules known.[84] Interestingly, the T_2 values measured for **3-Ni**-Py_2 and [Pd_{12}(**3-Ni**-Py_2)$_{24}$] are in the same range, 410 and 350 ns respectively. This suggests that bringing together multiple spin centers into a rigid capsule does not have a deleterious influence on the phase memory time. This is an important result as it suggests molecules containing multiple weakly interacting spins do not suffer huge decoherence effects, and hence have potential for applications in quantum technologies.

7. Conclusion

While the physical studies of single heterometallic rings are now extremely extensive, and the chemistry needed to synthesize rings of different sizes and shapes is well understood, the chemistry and physics of assemblies of such rings is only beginning. The single rings have proven to be excellent objects for studies including magnetization, EPR spectroscopy, and inelastic neutron

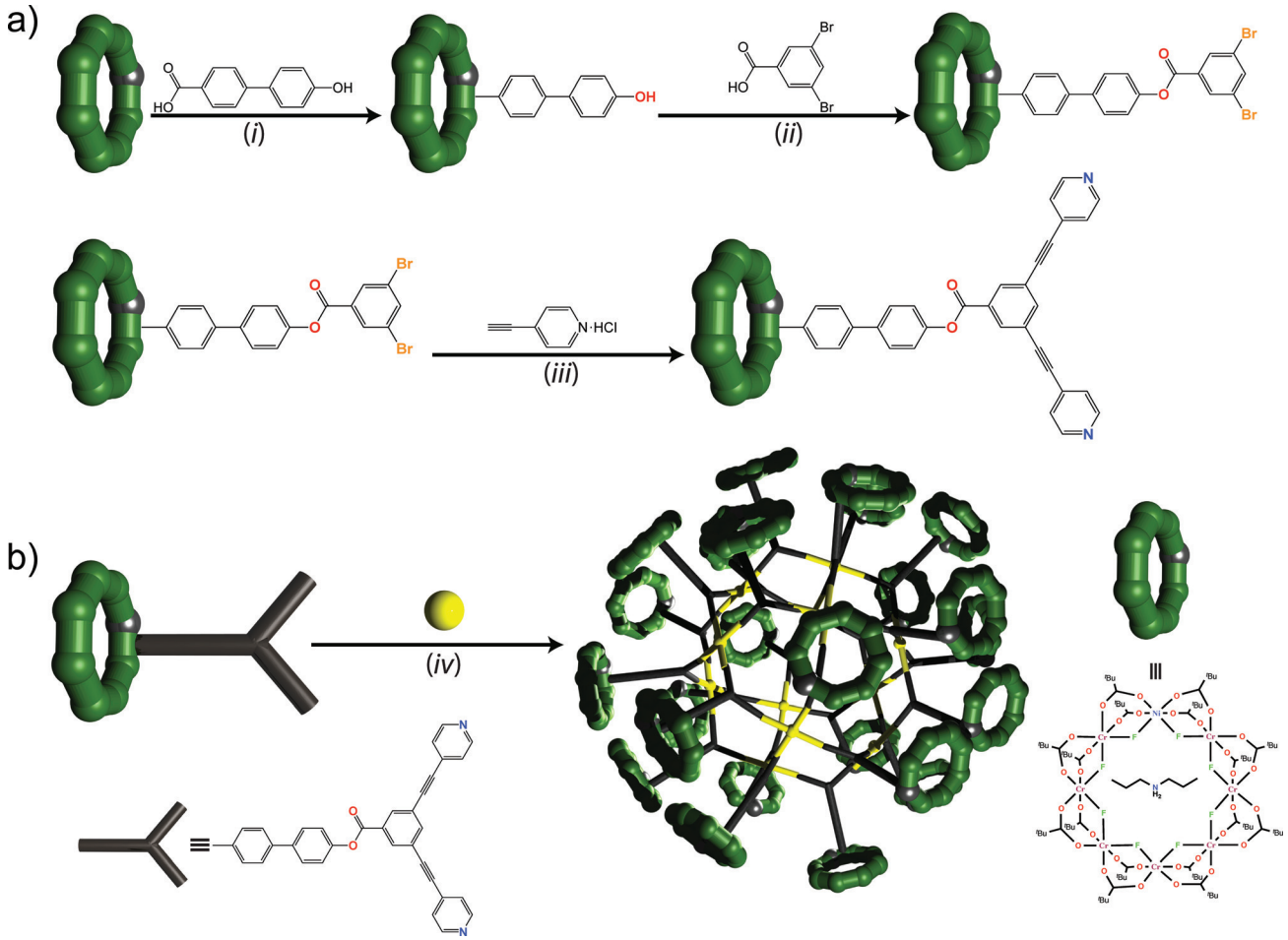

Figure 34. a) Synthetic steps taken to give **3-Ni**-Py_2. b) Self-assembly of the supramolecular 8 nm cage [Pd_{12}(**3-Ni**-Py_2)$_{24}$]. Modified from Ref. [84] with permission.

scattering, and these studies have allowed us to examine models for magnetism, such as the usefulness of the strong exchange limit, and have shown new physics, such as fluctuations of total spin at avoided crossings. This understanding will be vital as we try to understand the physics of the more extended molecular assemblies now being prepared. A key point is that the chemistry retains a classical elegance, using large symmetrical cage complexes as building blocks for still larger units.

Some future developments can be foreseen. Firstly, the proposal that such spin systems can be used in quantum information processing has many further challenges to meet. The key next challenge is to perform a simple algorithm; the experiments described above using pulsed EPR spectroscopy[66] show that the gate time in dimers of heterometallic rings is in the correct range for two-qubit gates to be performed. It is a vital next step, and one Takui and co-workers have made with organic radicals, to perform a CNOT gate.[86] The existence of $\{Ga_7Zn\}$ rings to act as diamagnetic hosts should allow orientated single crystals to be studied, and this has already been shown to be possible for single rings.[48] The chemistry to allow dimers of rings to be studied in a similar way will be challenging as the $\{Ga_7Zn\}$ rings are more reactive than $\{Cr_7M\}$ rings.

Concerning future new chemical reactions; there seems to be little limitation to what can be achieved. The key factor is the solubility and stability of the compounds involved. The presence of sixteen *tert*-butyl groups on the backbone of the **3-M** family of ligands creates coordination compounds that are highly soluble in the least-polar organic solvents. This opens up any bond forming reactions that can be done on any organic molecule, with the one exception that the rings are unstable in the presence of protic molecules and bases. Even in these cases though reactions are possible, but yields are reduced. 1D coordination polymers and 3D metal–organic frameworks have already been made featuring rings;[71,81] this area can be easily extended. Perhaps more exciting is the 8 nm $[Pd_{12}(\mathbf{3\text{-}Ni}\text{-}Py_2)_{24}]$ cage-of-cages we reported very recently. This is a huge molecule, and appears to be mono-dispersed in toluene solution.[84] We are targeting still larger molecules using the strategy developed to give this nano-object.

Acknowledgements

We are grateful to our many collaborators and group members who have made this work possible; there have been far too many over the last dozen years to list them all. The funds have been provided by the EPSRC(UK) through grants GR/57396/01, GR/T28652, EP/D05138X, EP/H011714, EP/J009377/1, EP/L018470/1, EP/K039547/1 and for funding for the National EPR Facility and Service. Some of the work described above was performed by students trained in the EPSRC Centre for Doctoral Training "NoWNANO"; NoWNANO supported G.F.S.W. We also thank the European Commission for support through Marie Curie Fellowships, and through a FET-OPEN project. The ILL and the Royal Society have also supported this work. R.E.P.W. is grateful to the Royal Society for a Wolfson Merit Award.

How to cite: *Angew. Chem. Int. Ed.* **2015**, *54*, 14244–14269
Angew. Chem. **2015**, *127*, 14450–14477

[1] K. L. Taft, C. D. Delfs, G. C. Papaefthymiou, S. Foner, D. Gatteschi, S. J. Lippard, *J. Am. Chem. Soc.* **1994**, *116*, 823–832.
[2] a) J. Schnack, M. Luban, *Phys. Rev. B* **2000**, *63*, 014418; b) O. Waldmann, *Phys. Rev. B* **2001**, *65*, 024424.
[3] O. Waldmann, T. C. Stamatatos, G. Christou, H. U. Güdel, I. Sheikin, H. Mutka, *Phys. Rev. Lett.* **2012**, *102*, 157202.
[4] a) J. Dreiser, O. Waldmann, C. Dobe, G. Carver, S. T. Ochsenbein, A. Sieber, H. U. Güdel, J. van Duijn, J. Taylor, A. Podlesnyak, *Phys. Rev. B* **2010**, *81*, 024408; b) J. Ummethum, J. Nehrkorn, S. Mukherjee, N. B. Ivanov, S. Stuiber, Th. Strässle, P. L. W. Tregenna-Pigott, H. Mutka, G. Christou, O. Waldmann, J. Schnack, *Phys. Rev. B* **2012**, *86*, 104403.
[5] N. V. Gerbeleu, Yu. T. Struchkov, G. A. Timco, A. S. Batsanov, K. M. Indrichan, G. A. Popovich, *Dokl. Akad. Nauk. SSSR* **1990**, *313*, 1459–1462.
[6] J. van Slageren, R. Sessoli, D. Gatteschi, A. A. Smith, M. Helliwell, R. E. P. Winpenny, A. Cornia, A.-L. Barra, A. G. M. Jansen, G. A. Timco, E. Rentschler, *Chem. Eur. J.* **2002**, *8*, 277–285.
[7] M. L. Baker, T. Guidi, S. Carretta, H. Mutka, G. Timco, E. J. L. McInnes, G. Amoretti, R. E. P. Winpenny, P. Santini, *Nat. Phys.* **2012**, *8*, 906–911.
[8] F. Meier, D. Loss, *Phys. Rev. B* **2001**, *64*, 224411.
[9] F. K. Larsen, E. J. L. McInnes, H. El Mkami, J. Overgaard, S. Piligkos, G. Rajaraman, E. Rentschler, A. A. Smith, G. M. Smith, V. Boote, M. Jennings, G. A. Timco, R. E. P. Winpenny, *Angew. Chem. Int. Ed.* **2003**, *42*, 101–105; *Angew. Chem.* **2003**, *115*, 105–109.
[10] M. Affronte, S. Carretta, G. A. Timco, R. E. P. Winpenny, *Chem. Commun.* **2007**, 1789–1797.
[11] a) S. Piligkos, E. Bill, D. Collison, E. J. L. McInnes, G. A. Timco, H. Weihe, R. E. P. Winpenny, F. Neese, *J. Am. Chem. Soc.* **2007**, *129*, 760–761; b) S. Piligkos, H. Weihe, E. Bill, F. Neese, H. El Mkami, G. M. Smith, D. Collison, G. Rajaraman, G. A. Timco, R. E. P. Winpenny, E. J. L. McInnes, *Chem. Eur. J.* **2009**, *15*, 3152–3167.
[12] F. K. Larsen, J. Overgaard, M. Christensen, G. J. McIntyre, G. Timco, R. E. P. Winpenny, *Acta Crystallogr. Sect. B* **2014**, *70*, 932–941.
[13] R. H. Laye, F. K. Larsen, J. Overgaard, C. A. Muryn, E. J. L. McInnes, E. Rentschler, V. Sanchez, H. U. Güdel, O. Waldmann, G. A. Timco, R. E. P. Winpenny, *Chem. Commun.* **2005**, 1125–1127.
[14] E. C. Sañudo, C. A. Muryn, M. A. Helliwell, G. A. Timco, W. Wernsdorfer, R. E. P. Winpenny, *Chem. Commun.* **2007**, 801–803.
[15] G. A. Timco, E. J. L. McInnes, R. G. Pritchard, F. Tuna, R. E. P. Winpenny, *Angew. Chem. Int. Ed.* **2008**, *47*, 9681–9684; *Angew. Chem.* **2008**, *120*, 9827–9830.
[16] E. Garlatti, M. A. Albring, M. L. Baker, R. J. Docherty, V. G. Sakai, H. Mutka, T. Guidi, G. F. S. Whitehead, R. G. Pritchard, G. A. Timco, F. Tuna, G. Amoretti, S. Carretta, P. Santini, G. Lorusso, M. Affronte, E. J. L. McInnes, D. Collison, R. E. P. Winpenny, *J. Am. Chem. Soc.* **2014**, *136*, 9763–9772.
[17] a) O. Cador, D. Gatteschi, R. Sessoli, F. K. Larsen, J. Overgaard, A.-L. Barra, S. J. Teat, G. A. Timco, R. E. P. Winpenny, *Angew. Chem. Int. Ed.* **2004**, *43*, 5196–5200; *Angew. Chem.* **2004**, *116*, 5308–5312; b) M. L. Baker, O. Waldmann, S. Piligkos, R. Bircher, O. Cador, S. Carretta, D. Collison, F. Fernandez-Alonso, E. J. L. McInnes, H. Mutka, A. Podlesnyak, F. Tuna, S. Ochsenbein, R. Sessoli, A. Sieber, G. A. Timco, H. Weihe, H. U. Güdel, R. E. P. Winpenny, *Phys. Rev. B* **2012**, *86*, 064405; c) A. Bianchi, S. Carretta, P. Santini, G. Amoretti, T. Guidi, Y. Qiu, J. R. D. Copley, G. Timco, C. Muryn, R. E. P. Winpenny, *Phys.*

Rev. B **2009**, *79*, 144422; d) T. Guidi, B. Gillon, S. A. Mason, E. Garlatti, S. Carretta, P. Santini, A. Stunault, R. Caciuffo, J. van Slageren, B. Klemke, A. Cousson, G. A. Timco, R. E. P. Winpenny, *Nat. Commun.* **2015**, im Druck.

[18] G. A. Timco, A. S. Batsanov, F. K. Larsen, C. A. Muryn, J. Overgaard, S. J. Teat, R. E. P. Winpenny, *Chem. Commun.* **2005**, 3649 – 3651.

[19] T. B. Faust, P. G. Heath, C. A. Muryn, G. A. Timco, R. E. P. Winpenny, *Chem. Commun.* **2010**, *46*, 6258 – 6260.

[20] A. B. Boeer, D. Collison, C. A. Muryn, G. A. Timco, F. Tuna, R. E. P. Winpenny, *Chem. Eur. J.* **2009**, *15*, 13150 – 13160.

[21] S. L. Heath, R. H. Laye, C. A. Muryn, R. Sessoli, R. Shaw, S. J. Teat, G. A. Timco, R. E. P. Winpenny, *Angew. Chem. Int. Ed.* **2004**, *43*, 6132 – 6135; *Angew. Chem.* **2004**, *116*, 6258 – 6261.

[22] F. K. Larsen, J. Overgaard, S. Parsons, E. Rentschler, G. A. Timco, A. A. Smith, R. E. P. Winpenny, *Angew. Chem. Int. Ed.* **2003**, *42*, 5978 – 5981; *Angew. Chem.* **2003**, *115*, 6160 – 6163.

[23] M. Shanmugam, L. P. Englehardt, F. K. Larsen, M. Luban, C. A. Muryn, E. J. L. McInnes, J. Overgaard, E. Rentschler, G. A. Timco, R. E. P. Winpenny, *Chem. Eur. J.* **2006**, *12*, 8267 – 8275.

[24] L. P. Engelhardt, C. A. Muryn, R. G. Pritchard, G. A. Timco, F. Tuna, R. E. P. Winpenny, *Angew. Chem. Int. Ed.* **2008**, *47*, 924 – 927; *Angew. Chem.* **2008**, *120*, 938 – 941.

[25] M. L. Baker, S. Piligkos, A. Bianchi, S. Carretta, D. Collison, J. J. W. McDouall, E. J. L. McInnes, H. Mutka, G. A. Timco, F. Tuna, P. Vadivelu, H. Weihe, H. U. Güdel, R. E. P. Winpenny, *Dalton Trans.* **2011**, *40*, 8533 – 8539.

[26] S. T. Ochsenbein, F. Tuna, M. Rancan, R. S. G. Davies, C. A. Muryn, O. Waldmann, R. Bircher, A. Sieber, G. Carver, H. Mutka, F. Fernandez-Alonso, A. Podlesnyak, L. P. Engelhardt, G. A. Timco, H. U. Güdel, R. E. P. Winpenny, *Chem. Eur. J.* **2008**, *14*, 5144 – 5158.

[27] M. Rancan, G. N. Newton, C. A. Muryn, R. G. Pritchard, G. A. Timco, L. Cronin, R. E. P. Winpenny, *Chem. Commun.* **2008**, 1560 – 1562.

[28] M. L. Baker, A. Bianchi, S. Carretta, D. Collison, R. Docherty, E. J. L. McInnes, A. McRobbie, C. A. Muryn, H. Mutka, S. Piligkos, M. Rancan, P. Santini, G. A. Timco, P. L. W. Tregenna-Piggott, F. Tuna, H. U. Güdel, R. E. P. Winpenny, *Dalton Trans.* **2011**, *40*, 2725 – 2734.

[29] A. McRobbie, A. R. Sarwar, S. Yeninas, H. Nowell, M. L. Baker, D. Allan, M. Luban, C. A. Muryn, R. G. Pritchard, R. Prozorov, G. A. Timco, F. Tuna, G. F. S. Whitehead, R. E. P. Winpenny, *Chem. Commun.* **2011**, *47*, 6251 – 6253.

[30] M. N. N. Hoshino, H. Nojiri, W. Wernsdorfer, H. Oshio, *J. Am. Chem. Soc.* **2009**, *131*, 15100 – 15101.

[31] H. Amiri, A. Lascialfari, Y. Furukawa, F. Borsa, G. A. Timco, R. E. P. Winpenny, *Phys. Rev. B* **2010**, *82*, 144421.

[32] R. Caciuffo, T. Guidi, S. Carretta, P. Santini, G. Amoretti, C. Mondelli, G. Timco, R. E. P. Winpenny, *Phys. Rev. B* **2005**, *71*, 174407.

[33] M. Affronte, T. Guidi, R. Caciuffo, S. Carretta, G. Amoretti, J. Hinderer, I. Sheikin, A. J. M. Jansen, A. A. Smith, R. E. P. Winpenny, J. van Slageren, D. Gatteschi, *Phys. Rev. B* **2003**, *68*, 104403.

[34] S. Carretta, P. Santini, G. Amoretti, M. Affronte, A. Ghirri, I. Sheikin, S. Piligkos, G. A. Timco, R. E. P. Winpenny, *Phys. Rev. B* **2005**, *72*, 060403.

[35] S. Carretta, P. Santini, G. Amoretti, T. Guidi, J. R. D. Copley, Y. Qiu, R. Caciuffo, G. Timco, R. E. P. Winpenny, *Phys. Rev. Lett.* **2007**, *98*, 167401.

[36] G. A. Timco, E. J. L. McInnes, R. E. P. Winpenny, *Chem. Soc. Rev.* **2013**, *42*, 1796 – 1806.

[37] M. N. Leuenberger, D. Loss, *Nature* **2001**, *410*, 789.

[38] F. Meier, J. Levy, D. Loss, *Phys. Rev. Lett.* **2003**, *90*, 047901.

[39] F. Troiani, A. Ghirri, M. Affronte, S. Carretta, P. Santini, G. Amoretti, S. Piligkos, G. Timco, R. E. P. Winpenny, *Phys. Rev. Lett.* **2005**, *94*, 207208.

[40] J. Lehmann, A. Gaita-Ariño, E. Coronado, D. Loss, *Nat. Nanotechnol.* **2007**, *2*, 312 – 317.

[41] A. Ardavan, O. Rival, J. J. L. Morton, S. J. Blundell, A. M. Tyryshkin, G. A. Timco, R. E. P. Winpenny, *Phys. Rev. Lett.* **2007**, *98*, 057201.

[42] a) C. J. Wedge, R. E. George, G. A. Timco, F. Tuna, S. Rigby, E. J. L. McInnes, R. E. P. Winpenny, S. J. Blundell, A. Ardavan, *Phys. Rev. Lett.* **2012**, *108*, 107204; b) D. Kaminski, A. L. Webber, C. J. Wedge, J. Liu, G. A. Timco, I. J. Vitorica-Yrezabal, E. J. L. McInnes, R. E. P. Winpenny, A. Ardavan, *Phys. Rev. B* **2014**, *90*, 184419.

[43] C. Schlegel, J. van Slageren, M. Manoli, E. K. Brechin, M. Dressel, *Phys. Rev. Lett.* **2008**, *101*, 147203.

[44] S. Bertaina, S. Gambarelli, T. Mitra, B. Tsukerblat, A. Müller, B. Barbara, *Nature* **2008**, *453*, 203 – 206.

[45] M. Warner, S. Din, I. S. Tupitsyn, G. W. Morley, A. M. Stoneham, J. A. Gardner, Z. Wu, A. J. Fisher, S. Heutz, C. W. M. Kay, G. Aeppli, *Nature* **2013**, *503*, 504 – 508.

[46] K. Bader, D. Dengler, S. Lenz, B. Endeward, S. D. Jiang, P. Neugebauer, J. van Slageren, *Nat. Commun.* **2014**, *5*, 5304.

[47] M. J. Graham, J. M. Zadrozny, M. Shiddiq, J. S. Anderson, M. S. Fataftah, S. Hill, D. E. Freedman, *J. Am. Chem. Soc.* **2014**, *136*, 7623 – 7626.

[48] F. Moro, D. Kaminski, F. Tuna, G. F. S. Whitehead, G. A. Timco, D. Collison, R. E. P. Winpenny, A. Ardavan, E. J. L. McInnes, *Chem. Commun.* **2014**, *50*, 91 – 93.

[49] C. Schlegel, J. van Slageren, G. Timco, R. E. P. Winpenny, M. Dressel, *Phys. Rev. B* **2011**, *83*, 134407.

[50] E. Micotti, Y. Furukawa, A. Lascialfari, F. Borsa, S. Carretta, A. Cornia, M. H. Julien, M. Horvatic, G. A. Timco, R. E. P. Winpenny, *Phys. Rev. Lett.* **2006**, *97*, 267204.

[51] C. M. Casadei, L. Bordonali, Y. Furukawa, F. Borsa, E. Garlatti, A. Lascialfari, S. Carretta, S. Sanna, G. Timco, R. E. P. Winpenny, *J. Phys. Condens. Matter* **2012**, *24*, 406002.

[52] L. Bordonali, E. Garlatti, C. M. Casadei, Y. Furukawa, A. Lascialfari, S. Carretta, F. Troiani, G. Timco, R. E. P. Winpenny, F. Borsa, *J. Chem. Phys.* **2014**, *140*, 144306.

[53] C. Martin, L. Engelhardt, M. L. Baker, G. A. Timco, F. Tuna, R. E. P. Winpenny, P. L. W. Tregenna-Piggott, M. Luban, R. Prozorov, *Phys. Rev. B* **2009**, *80*, 100407.

[54] L. Engelhardt, C. Martin, R. Prozorov, M. Luban, G. A. Timco, R. E. P. Winpenny, *Phys. Rev. B* **2009**, *79*, 014404.

[55] M. Mannini, F. Pineider, C. Danielle, F. Totti, L. Sorace, P. Sainctavit, M. A. Arrio, E. Otero, L. Joly, J. C. Cezar, A. Cornia, R. Sessoli, *Nature* **2010**, *468*, 417 – 421.

[56] a) A. L. Rizzini, C. Krull, T. Balashov, J. Kavich, A. Mugarza, P. Miedema, P. Thakur, V. Sessi, S. Klyatskaya, M. Ruben, S. Stepanow, P. Gambardella, *Phys. Rev. Lett.* **2011**, *107*, 177205; b) D. Klar, A. Candini, L. Joly, S. Klyatskaya, B. Krumme, P. Ohresser, J. P. Kappler, M. Ruben, H. Wende, *Dalton Trans.* **2014**, *43*, 10686 – 10689.

[57] T. Komeda, H. Isshiki, J. Liu, Y. F. Zhang, N. Lorente, K. Katoh, B. K. Breedlove, M. Yamashita, *Nat. Commun.* **2011**, *2*, 217.

[58] V. A. Milway, S. M. T. Abedin, V. Niel, T. L. Kelly, L. N. Dawe, S. K. Dey, D. W. Thompson, D. O. Miller, M. S. Alam, P. Müller, L. K. Thompson, *Dalton Trans.* **2006**, 2835 – 2851.

[59] V. Corradini, F. Moro, R. Biagi, V. De Renzi, U. del Pennino, V. Bellini, S. Carretta, P. Santini, V. A. Milway, G. Timco, R. E. P. Winpenny, M. Affronte, *Phys. Rev. B* **2009**, *79*, 144419.

[60] A. Ghirri, V. Corradini, C. Cervetti, A. Candini, U. del Pennino, G. A. Timco, R. G. Pritchard, C. A. Muryn, R. E. P. Winpenny, M. Affronte, *Adv. Funct. Mater.* **2010**, *20*, 1552 – 1560.

[61] A. Ghirri, V. Corradini, V. Bellini, R. Biagi, U. del Pennino, V. De Renzi, J. Cezar, C. Muryn, G. A. Timco, R. E. P. Winpenny, M. Affronte, *ACS Nano* **2011**, *5*, 7090 – 7099.
[62] T. B. Faust, V. Bellini, A. Candini, S. Carretta, G. Lorusso, D. R. Allan, L. Carthy, D. Collison, R. J. Docherty, J. Kenyon, J. Machin, E. J. L. McInnes, C. A. Muryn, H. Nowell, R. G. Pritchard, S. J. Teat, G. A. Timco, F. Tuna, G. F. S. Whitehead, W. Wernsdorfer, M. Affronte, R. E. P. Winpenny, *Chem. Eur. J.* **2011**, *17*, 14020 – 14030.
[63] T. B. Faust, F. Tuna, G. A. Timco, M. Affronte, V. Bellini, W. Wernsdorfer, R. E. P. Winpenny, *Dalton Trans.* **2012**, *41*, 13626 – 13631.
[64] A. Candini, G. Lorusso, F. Troiani, A. Ghirri, S. Carretta, P. Santini, G. Amoretti, C. Muryn, F. Tuna, G. Timco, E. J. L. McInnes, R. E. P. Winpenny, W. Wernsdorfer, M. Affronte, *Phys. Rev. Lett.* **2010**, *104*, 037203.
[65] V. Bellini, G. Lorusso, A. Candini, W. Wernsdorfer, T. B. Faust, G. A. Timco, R. E. P. Winpenny, M. Affronte, *Phys. Rev. Lett.* **2011**, *106*, 227205.
[66] A. Ardavan, A. Bowen, A. Fernandez, A. Fielding, D. Kaminski, F. Moro, C. A. Muryn, M. D. Wise, A. Ruggi, E. J. L. McInnes, K. Severin, G. A. Timco, C. R. Timmel, F. Tuna, G. F. S. Whitehead, R. E. P. Winpenny, arXiv: 1510.01694. *NPJ Quantum Information*, accepted.
[67] M. D. Wise, A. Ruggi, M. Pascu, R. Scopelliti, K. Severin, *Chem. Sci.* **2013**, *4*, 1658 – 1662.
[68] M. Affronte, I. Casson, M. Evangelisti, A. Candini, S. Carretta, C. A. Muryn, S. J. Teat, G. A. Timco, W. Wernsdorfer, R. E. P. Winpenny, *Angew. Chem. Int. Ed.* **2005**, *44*, 6496 – 6500; *Angew. Chem.* **2005**, *117*, 6654 – 6658.
[69] C.-F. Lee, D. A. Leigh, R. G. Pritchard, D. Schultz, S. J. Teat, G. A. Timco, R. E. P. Winpenny, *Nature* **2009**, *458*, 314 – 318.
[70] B. Ballesteros, T. B. Faust, C. F. Lee, D. A. Leigh, C. A. Muryn, R. G. Pritchard, D. Schultz, S. J. Teat, G. A. Timco, R. E. P. Winpenny, *J. Am. Chem. Soc.* **2010**, *132*, 15435 – 15444.
[71] G. F. S. Whitehead, B. Cross, L. Carthy, V. A. Milway, H. Rath, A. Fernandez, S. L. Heath, C. A. Muryn, R. G. Pritchard, S. J. Teat, G. A. Timco, R. E. P. Winpenny, *Chem. Commun.* **2013**, *49*, 7195 – 7197.
[72] S. J. Loeb, *Chem. Commun.* **2005**, 1511 – 1518.
[73] P. Santini, S. Carretta, F. Troiani, G. Amoretti, *Phys. Rev. Lett.* **2011**, *107*, 230502.
[74] H. Rath, G. A. Timco, V. Corradini, A. Ghirri, U. del Pennino, A. Fernandez, R. G. Pritchard, C. A. Muryn, M. Affronte, R. E. P. Winpenny, *Chem. Commun.* **2013**, *49*, 3404 – 3406.
[75] A. Fernandez, E. M. Pineda, J. Ferrando-Soria, E. J. L. McInnes, G. A. Timco, R. E. P. Winpenny, *Chem. Commun.* **2015**, *51*, 11126.
[76] P. R. Ashton, I. Baxter, S. J. Cantrill, M. C. T. Fyfe, P. T. Glink, J. F. Stoddart, A. J. P. White, D. J. Williams, *Angew. Chem. Int. Ed.* **1998**, *37*, 1294; *Angew. Chem.* **1998**, *110*, 1344.
[77] A. Fernandez, E. M. Pineda, C. A. Muryn, S. Sproules, F. Moro, G. A. Timco, E. J. L. McInnes, R. E. P. Winpenny, *Angew. Chem. Int. Ed.* **2015**, *54*, 10858; *Angew. Chem.* **2015**, *127*, 11008.
[78] G. A. Timco, S. Carretta, F. Troiani, F. Tuna, R. G. Pritchard, E. J. L. McInnes, A. Ghirri, A. Candini, P. Santini, G. Amoretti, M. Affronte, R. E. P. Winpenny, *Nat. Nanotechnol.* **2009**, *4*, 173 – 178.
[79] A. Chiesa, G. F. S. Whitehead, S. Carretta, L. Carthy, G. A. Timco, S. J. Teat, G. Amoretti, E. Pavarini, R. E. P. Winpenny, P. Santini, *Sci. Rep.* **2014**, *4*, 7423.
[80] G. F. S. Whitehead, F. Moro, G. A. Timco, W. Wernsdorfer, S. J. Teat, R. E. P. Winpenny, *Angew. Chem. Int. Ed.* **2013**, *52*, 9932 – 9935; *Angew. Chem.* **2013**, *125*, 10116 – 10119.
[81] G. F. S. Whitehead, J. Ferrando-Soria, L. G. Christie, N. F. Chilton, G. A. Timco, F. Moro, R. E. P. Winpenny, *Chem. Sci.* **2014**, *5*, 235 – 239.
[82] G. F. S. Whitehead, S. J. Teat, K. J. Gagnon, G. A. Timco, R. E. P. Winpenny, *Chem. Commun.* **2015**, *51*, 3533 – 3536.
[83] S. F. Lincoln, *Helv. Chim. Acta* **2005**, *88*, 523 – 545.
[84] J. Ferrando-Soria, A. Fernandez, E. M. Pineda, S. A. Varey, R. W. Adams, I. J. Vitorica-Yrezabal, F. Tuna, G. A. Timco, C. A. Muryn, R. E. P. Winpenny, *J. Am. Chem. Soc.* **2015**, *137*, 7644.
[85] a) S. Leininger, B. Olenyuk, P. J. Stang, *Chem. Rev.* **2000**, *100*, 853; b) S. R. Seidel, P. J. Stang, *Acc. Chem. Res.* **2002**, *35*, 972; c) M. Fujita, M. Tominaga, A. Hori, B. Therrien, *Acc. Chem. Res.* **2005**, *38*, 371.
[86] S. Nakazawa, S. Nishida, T. Ise, T. Yoshino, N. R. Mori, D. Rahimi, K. Sato, Y. Morita, K. Toyota, D. Shiomi, M. Kitagawa, H. Hara, P. Carl, P. Höfer, T. Takui, *Angew. Chem. Int. Ed.* **2012**, *51*, 9860; *Angew. Chem.* **2012**, *124*, 9998.

Received: April 13, 2015
Published online: October 13, 2015

